

Column-to-Beam Moment Capacity Ratio of Framed Building

Abhijit Mistri



Department of Civil Engineering
National Institute of Technology, Rourkela
Odisha, India – 769008

Column-to-Beam Moment Capacity Ratio of Framed Building

A Thesis submitted in partial fulfillment of
the requirements for the award of the degree of

Master of Technology

in

Structural Engineering

Submitted to

National Institute of Technology Rourkela

by

Abhijit Mistri

(Roll No. 214CE2058)

*Based on research carried out
under the supervision of
Prof. Pradip Sarkar*



Department of Civil Engineering
National Institute of Technology Rourkela
Odisha, India – 769 008
May 2016

*Dedicated to
my family*



Department of Civil Engineering
National Institute of Technology Rourkela
Rourkela-769 008 , Odisha , India. www.nitrkl.ac.in

Prof. Pradip Sarkar
Associate Professor

May , 2016

Certificate

This is to certify that the work in the thesis entitled *Column-to-Beam Moment Capacity Ratio of Framed Building* by *Abhijit Mistri*, bearing Roll No. *214CE2058*, is a record of an original research work carried out by him under my supervision and guidance in partial fulfillment of the requirements for the award of the degree of *Master of Technology in Structural Engineering, Department of Civil Engineering*. The contents of this thesis, have not been submitted in full or in parts, to any other Institute or University in India or abroad for the award of any other degree elsewhere to the best of my knowledge.

Pradip Sarkar

Acknowledgment

Contributions from some persons in numerous ways helped this research work and they deserve special thanks. It is a pleasure to express my gratitude to all of them.

First of all, I would like to express my sincere gratitude to my supervisor Prof. Pradip Sarkar for enlightening me for this research work. His valuable guidance, support, consistent encouragement and immense knowledge in the subjects helped me a lot throughout this course of my M.Tech project work, introducing real life civil engineering work through consultancy project and also in writing this thesis. Besides my advisor, I would like to thank Prof Robin Davis P for his timely co-operations and guidance for this project work. He has always been the friend, philosopher and co-guide for me. I also extend my sincere thanks to Prof. Shishir Kumar Sahu, Head of the department of civil engineering for his encouragement and advices for research and my conference presentation.

I am very grateful to the PhD seniors Haran Pragalath D.C., Avadhoot Bhosale, Kirtikanta Sahoo for clarifying many technical doubts and solving the difficulties using software and also technical paper writing.

I am also very thankful to my friend Prateek Kumar Dhir, Debasish Rath and classmates of structural engineering for being with me throughout the year and encouraging me to move ahead.

Finally I would like thank my parents and my younger brother Suvajit Mistri from the bottom of my heart for their unconditional love, constant help, moral support and inspirations all throughout my life. Without their support nothing would have been possible. I am greatly indebted to them.

Abhijit Mistri

Declaration of Originality

I, *Abhijit Mistri*, Roll Number *214CE2058* hereby declare that this thesis entitled *Column-to-Beam Moment Capacity Ratio of Framed Building* presents my original work carried out as a master student of *National Institute of Technology Rourkela*, to the best of my knowledge, contains no material previously published or written by another person, nor any material presented by me for the award of any degree or diploma of National Institute of Technology Rourkela or any other institution of World. Any contribution made to this research by others, with whom I have worked at NIT Rourkela or elsewhere, is explicitly acknowledged in the thesis. Works of other authors cited in this thesis have been duly acknowledged under the chapter Reference.

I am fully aware that in case of any non-compliance detected in future, the Senate of National Institute of Technology Rourkela may withdraw the degree awarded to me on the basis of the present thesis.

Abhijit Mistri
Roll No. 214CE2058
Structural Engineering

Abstract

Capacity design philosophy is the basis of behind the strong column weak beam concept for the improvement of earthquake resistant design. Damages at some in some pre-determined structural members may allowed in the earthquake-resistant design philosophy in order to have a good global behaviour of the building.

In order to ensure a favorable failure mode, design codes recommend minimum value of Moment Capacity Ratio (MCR) which is defined as the ratio of summation of column moment capacity to summation of beam moment capacity at a particular beam-column joint. During cyclic earthquake loading column experience a range of axial force due to various combinations of load, and unlike beam, column does not have a unique moment capacity. That makes the calculation of MCR cumbersome.

There are discrepancies among the major international codes with regard to MCR. Indian standard codes for design of RC framed buildings are silent on this aspect. Draft 13920 (2014) code suggests a value of MCR similar to other international codes without proper theoretical basis. Hence a rational study is required on the values of MCR. A computationally attractive procedure for calculating flexural capacity of column developed for determining MCR at a beam-column joint. To reach at an appropriate and acceptable MCR for capacity design of RC framed building reliability based approach is done.

This research deals with the fragility and reliability analysis of four storey RC frames designed using various values of MCR ranging from 1.0 to 3.2. The RC frames are designed as per IS 1893 (2002) for all seismic zones. Hazard curves required of various seismic location in India (like zone II, III, IV and V) has been selected from National Disaster Management Authority, Government of India. Seismic risk assessment of all the designed buildings is conducted and based on the achieved Reliability Index and the Target Reliability Index minimum value of MCR is suggested.

Keywords : *earthquake resistant design, MCR, PSDMs, fragility analysis, reliability index*

Contents

| | |
|---|------------|
| <i>Certificate</i> | <i>iii</i> |
| <i>Acknowledgement</i> | <i>iv</i> |
| <i>Declaration of Originality</i> | <i>v</i> |
| <i>Abstract</i> | <i>vi</i> |
| <i>List of Figures</i> | <i>ix</i> |
| <i>List of Tables</i> | <i>xi</i> |
| 1 Background and Motivation | 1 |
| 1.1 Introduction | 1 |
| 1.2 Concept of Strong Column Weak Beam | 2 |
| 1.3 Reasearch Gap and Motivation | 4 |
| 1.4 Objectives of Present Study | 5 |
| 1.5 Methodology | 5 |
| 1.6 Organization of Thesis | 6 |
| 2 Review of Literature | 7 |
| 2.1 General | 7 |
| 2.2 Capacity Based Design of RC Framed Structure | 7 |
| 2.3 Review of Major International Codes | 9 |
| 2.4 Review on Pushover Analysis | 11 |
| 2.5 Previous Research on Seismic Risk Assessment | 12 |
| 2.6 Summary | 13 |

| | | |
|----------|--|-----------|
| 3 | <i>Effect of MCR on the Seismic Performance of Buildings</i> | 14 |
| 3.1 | Introduction | 14 |
| 3.2 | Pushover Analysis Procedure (FEMA 356) | 14 |
| 3.3 | Selected Frames | 15 |
| 3.4 | Summary | 17 |
| 4 | <i>Development of Simplified Procedure for Estimating MCR</i> | 18 |
| 4.1 | Introduction | 18 |
| 4.2 | Range of Normalized Axial Force in Buildings | 18 |
| 4.3 | MCR Using the Design Charts of SP-16 | 24 |
| 4.4 | Minimum Moment Capacity Analytical Method | 26 |
| 4.5 | Minimum Moment Capacity Column - SP16 v/s Analytical Method | 30 |
| 4.6 | Summary | 33 |
| 5 | <i>Effect of MCR on Fragility and Reliability</i> | 34 |
| 5.1 | General | 34 |
| 5.2 | Earthquake Risk Assessment | 34 |
| 5.2.1 | Seismic Hazard Curves | 36 |
| 5.2.2 | Development of Fragility Curves | 36 |
| 5.3 | Sampling of Variables | 40 |
| 5.4 | Probabilistic Seismic Demand Models | 41 |
| 5.5 | Fragility Curves | 41 |
| 5.6 | Reliability Curves | 44 |
| 5.7 | Summary | 47 |
| 6 | <i>Conclusions</i> | 48 |
| 6.1 | Summary and Conclusions | 48 |
| 6.2 | Future Research Scope | 49 |
| | <i>Appendix-A</i> | 50 |
| | <i>Appendix-B</i> | 52 |

List of Figures

| | | |
|--------------|---|----|
| Figure 1.1: | Picture of Bhuj Earthquake damaged building, Gujrat, India (www.google.com) | 1 |
| Figure 1.2: | Picture of failure in beam column joint after an event of earthquake. (a) (www.db.concretcoalition.org), (b) (www.thaiengineering.com) | 2 |
| Figure 3.1: | Typical Moment-Rotation curve showing performance levels | 15 |
| Figure 3.2: | Global hinge status at 0.84 m displacement | 16 |
| Figure 3.3: | Comparison of pushover curve at 0.84 m displacement | 16 |
| Figure 4.1: | Column axial force for four-storey building | 20 |
| Figure 4.2: | Column axial force for six-storey building | 21 |
| Figure 4.3: | Column axial force for eight-storey building | 22 |
| Figure 4.4: | Column axial force for ten-storey building | 23 |
| Figure 4.5: | Column axial force range (typical) for interior column shown in design chart of SP 16 | 25 |
| Figure 4.6: | Analysis of design strength of a rectangular section under eccentric compression (a) neutral axis within the section, (b) neutral axis outside of the section (Pillai and Menon, 2015) | 27 |
| Figure 4.7: | 3D view of Block-D, staff quarter Jamshedpur (G+2) | 31 |
| Figure 4.8: | Plan view of Block-D, staff quarter Jamshedpur (G+2) | 31 |
| Figure 4.9: | 3D view of Block-A, Jamshedpur Hospital Building (G+4) | 32 |
| Figure 4.10: | Plan view of Block-A, Jamshedpur Hospital Building (G+4) | 32 |
| Figure 5.1: | Different Hazard level at the selected location (http://www.ndma.gov.in/en/) | 36 |
| Figure 5.2: | Time history data (http://strongmotioncenter.org/) | 40 |
| Figure 5.3: | PSDM model for the selected buildings under given earthquake | 41 |
| Figure 5.4: | Fragility curve of IO for various MCR | 42 |
| Figure 5.5: | Fragility curve of SD for various MCR | 43 |
| Figure 5.6: | Fragility curve of CP for various MCR | 43 |
| Figure 5.7: | Reliability curve of CP for Seismic Zone II | 44 |

List of Tables

| | | |
|-----|--|----|
| 1.1 | Minimum MCR recommended by design codes and published literature | 5 |
| 3.1 | Details of parameters considered for design | 16 |
| 4.1 | Column axial force for four-storey building | 20 |
| 4.2 | Column axial force for six-storey building | 21 |
| 4.3 | Column axial force for eight-storey building | 22 |
| 4.4 | Column axial force for Ten-storey building | 23 |
| 4.5 | Column Moment Capacities | 25 |
| 4.6 | Validation of computer programs with Pillai and Menon, 2015 | 29 |
| 4.7 | Result of existing building Block-D | 30 |
| 4.8 | Result of existing building Block-A | 33 |
| 5.1 | Different Hazard level at selected location | 37 |
| 5.2 | Damage limits and dispersion associated with various structural performance levels | 39 |
| 5.3 | Details of random variables used in LHS scheme | 40 |
| 5.4 | Target Reliability for IO of various hazard location | 45 |
| 5.5 | Target Reliability for SD of various hazard location | 45 |
| 5.6 | Target Reliability for CP of various hazard location | 46 |
| 5.7 | Suggested MCR for various hazard Location | 46 |
| 6.1 | Seismic Hazard Zone V | 50 |
| 6.2 | Seismic Hazard Zone IV | 50 |
| 6.3 | Seismic Hazard Zone III | 51 |
| 6.4 | Seismic Hazard Zone II | 51 |
| 6.5 | Column Section Details for Estimating MCR | 52 |
| 6.6 | Floor Beam Section Details for Estimating MCR | 52 |
| 6.7 | Roof Beam Section Details for Estimating MCR | 52 |

Chapter 1

Background and Motivation

1.1 Introduction

A lot of research attention was devoted to earthquake safety of buildings in India after the massive January 26, 2001 Bhuj Earthquake. The earthquake ranks as one of the most destructive events recorded so far in India in terms of death of people, destroy or damage of infrastructure and devastation in the last fifty years. Fig. 1.1 shows a damaged building in Buhj, Gujrat, India.



Figure 1.1: Picture of Bhuj Earthquake damaged building, Gujrat, India
(www.googlelet.com)

Many of the failures of RC framed buildings in Bhuj Earthquake are attributed to the weak column strong beam joints. Weak beam-column joint is measured to be one of the possibly weaker components related to a structure when that structure is subjected to dynamic loading. A number of examples are there throughout the world that buildings are failing globally through weak beam-to-column joints. Figs. 1.2(a) and 1.2(b) shows some failure in beam column joints after an event of earthquake. Such weak beam column joints failure pattern need to be given individual attention.



(a)

(b)

Figure 1.2: Picture of failure in beam column joint after an event of earthquake. (a) (www.db.concretcoalition.org), (b) (www.thaiengineering.com)

1.2 Concept of Strong Column Weak Beam

Capacity design philosophy suggested by Paulay and Priestley (1992) is the basis of behind the strong column weak beam concept for the improvement of earthquake resistant design of structure [1]. In this philosophy, structural design is formulated on the stress resultants achieved from linear structural analysis subjected to international code specified design lateral forces as well as equilibrium compatible stress

resultants achieved from predetermined collapse mechanism. Damages at some in some pre-determined structural members may allowed in the earthquake-resistant design philosophy in order to have a good global behaviour of the building. The flexural strengths of structural-members are determined on the basis of global response of the structure to earthquake forces. For this purpose, within a structural system the ductile components can be permitted to yield whereas the brittle components are not permitted to yield and should have sufficiently higher strength.

The capacity design philosophy sets strength hierarchy first at the structural component level and then at the global structure level. In order to satisfy the strong column beam weak philosophy, the strength of column shall be more than strength of beam and it can be written as,

$$M_c \geq M_b \quad (1.1)$$

Where, M_c and M_b are moment carrying capacities of column and beam meeting at a particular joint respectively. This strong-column / weak-beam design philosophy ensures good ductility and a desirable collapse mechanism in the building. For ensuring good global energy-dissipation with less degradation of capacity at that connections the failure mode where in the beams form hinges is usually considered to be the most favourable mode. The motives for implementing this Strong Column Weak Beam (SCWB) design are discussed below:

- Beam supports the floor surface but column supports to take the weight of entire building above it. So failure of the column is more critical than beam.
- Failure of column is global failure and failure of beam is local failure in a building structure.
- If a beam is designed to be the weakest at a specific beam-column-joint then other failure of that joint (like shear failure of joint core, anchorage failure, spalling of concrete,) also can be neglected.
- Beam can be designed to be more ductile than columns with lesser compression loads on them, and can absorb large amount of energy through inelastic actions.
- Similarly to the example of a chain link for capacity design approach proposed by (Murthy et al., 2013), to make a structural system ductile the weakest component should be the beam. [2].

- During an event of earthquake the inertia force encouraged in the structural system cause it to sway laterally. Over the building height the distribution of damages and the lateral drift of the structure are related.
- Drift value is generally high for weak column and so the damages to concentrate in one or a few stories only and if the drift capacity of the columns is exceeded the limit then it is of greater consequence. To obtain more uniformly drift distribution over the building height columns should be stiff and strong spine, therefore reducing the occurrences of localized damages of the structure.

1.3 Research Gap and Motivation

In order to ensure a favorable failure mode, design codes recommend minimum value of Moment Capacity Ratio (MCR) which is defined as the ratio of summation of column moment capacity to summation of beam moment capacity at a particular beam-column joint. Mathematically the expression can be written as,

$$MCR = \frac{\sum M_c}{\sum M_b} \quad (1.2)$$

Failure of several international code compliant building structure during previous earthquake by development of storey mechanism increases concern on the applicability of the code requirements.

Table 1.1 shows the values of MCR by various codes and published literature, where Ω is over strength factor for beams. Discrepancies among the major international codes with regard to MCR can be seen from the table. Indian standard codes for design of RC framed buildings are silent on this aspect. Draft 13920 (2014) code suggests a value of MCR similar to other international codes without proper theoretical basis [3]. Hence a rational study is required on the values of MCR. This is the fundamental motivation of this present research.

The MCR is defined as the ratio of cumulative column moment capacity to cumulative beam moment capacity framing to a particular joint. Although this appears to be a simple, procedure for calculation of column moment capacity is a matter of concern for the design office as it depends on the axial force level the column is subjected to. During cyclic earthquake loading column experience a range of axial force due to various combinations of load, and unlike beam, column does not have a unique moment capacity. That makes the calculation of MCR cumbersome.

Table 1.1: Minimum MCR recommended by design codes and published literature

| Documents | MCR |
|------------------------|--------------|
| Uma and Jain, 2006 | 1.1 |
| ACI 318M-14 | 1.2 |
| NZS3101:1995 | 1.4 Ω |
| EN1998-1:2003 | 1.3 |
| IS 13920 (draft): 2014 | 1.4 |

1.4 Objectives of Present Study

Based on the above discussions presented in the previous section, the primary objectives of the present study are as follows:

1. To study the behaviour of buildings designed for various MCR values
2. To develop a computationally simple procedure for calculating the nominal design strength of column to be used in determining MCR at a beam-column joint.
3. To reach at an appropriate and acceptable MCR for capacity design of RC framed building using reliability based approach.

1.5 Methodology

The methodology functioned out to attain the above- declared objectives are as follows:

- a. To carry out detailed literature review on MCR at beam-column joint.
- b. To select building geometries with different heights and base widths, analyse and design to conduct equivalent static analysis..
- c. To study the behavior of buildings designed with various MCR
- d. To find out the possible range of axial loading in the columns (with respect to its maximum axial load carrying capacity) and to develop a computationally

attractive procedure for calculating flexural capacity of column to be used in determining MCR at a beam-column joint.

- e. To select building models with various MCRs (ranging from 1.0 to 3.2).
- f. To conduct reliability analysis and to determine the reliability of various buildings designed as per different MCRs.

1.6 Organization of Thesis

A brief introduction of strong column weak beam design philosophy, research gap, motivation, objectives and methodology are discussed in this introductory chapter (Chapter 1).

Chapter 2 is devoted to the state of the art literature review on different subjects related to beam column joints. An overview of existing international design guidelines for strong column weak beam philosophy. Review on pushover analysis, fragility analysis, and reliability analysis are also provided.

Chapter 3 discusses the global and local failure mechanism of RC framed building for various MCR using pushover analysis.

Chapter 4 is devoted for development of a simplified procedure for calculating the MCR at a beam-column joint.

Chapter 5 discusses the reliability analysis of buildings designed with various MCR values.

Finally the conclusion of the present research is represented in Chapter 6.

Chapter 2

Review of Literature

2.1 General

This chapter deals with the current state of the art in the capacity based design approach suggested by major international design codes along with published literature. It starts with a review of published literature followed by a review of appropriate international design codes of practice on capacity based design of RC framed structure. The present study uses pushover analysis and seismic performance assessment using SAC-FEMA method. The methodology of pushover analysis as well as seismic performance assessment using SAC-FEMA method are explained in this Chapter.

2.2 Capacity Based Design of RC Framed Structure

In recent earthquakes all over the world the behaviour of reinforced concrete moment resisting frame structures has highlighted the consequences of poor performance of beam column joints. A huge number of research has carried out to understand the complex mechanisms and safe behaviour of beam column joints.

Sugano et al., (1988) showed analytical and experimental investigation on thirty-storey Reinforced Concrete framed building in Japan and developed design thought to ensure a better collapse mechanism as well as to observe the ductility of plastic hinges [4]. It was assured by analytical and experimental investigation

that the designed structure would have sufficient margin of seismic capacity as well as seismic performance.

Nakashima (2000) examined for steel building for ensuring column-elastic behavior by keeping the column over strength factor [5]. For ensuring column-elastic response, with increase in ground motion amplitude column over strength factor increases.

Dooley and Bracci (2001) reported that according to design provision of Japan building code (BCJ 2004) a minimum value for column over-strength factor (COF) 1.5 is suggested for cold-formed square tube structures in Japan [6]. A COF of 1.0 is considered in the seismic provision of structural steel building (ANSI/AISC 341-2005). Countries like New Zealand and Mexico adopted a COF ranging from 1.5 to 2.0. Performance of two case study buildings (three and six stories) with varying strength ratios (ranging from 0.8 to 2.4) were assessed considering the column-to-beam stiffness ratio as a parameter. The study proposed that a minimum strength ratio of 2.0 is more appropriate to prevent the formation of a story mechanism under design seismic loading.

Dominant collapse modes of the frames is investigated by many studies. Hibino and Ichinose (2005) studied the effect of flexural strength ratio of column-to-beam in fish-bone-type steel moment frames on the global energy dissipation. Number of stories, strengths of columns and beams and earthquake ground motion considered as the major parameters [7].

Jain et al., (2006) projected that, at beam-column joint when a reinforced concrete moment resisting frame is subjected to seismic loads, the summation of moment of resistances of columns should be always greater than or equal to 1.1 times the summation of moment of resistance of beams framing into it [8]. Mathematically,

$$\sum M_c \geq 1.1 \sum M_b \quad (2.1)$$

It was also suggested for the provision of confinement bars in the connection of wide beam column joints

George and Varghese (2012) concluded that the pushover analysis is a relatively simple way to explore the non-linear behaviour of buildings, the behaviour of properly detailed reinforced concrete frame building is adequate as indicated by

the intersection of the demand and capacity curves and the distribution of hinges in the beams and the columns [9]. The causes of failure of reinforced concrete during the Bhuj earthquake (2001) may be attributed to the quality of the materials used and also to the fact that most of buildings constructed in that region are of strong beam and weak column type and not to the intrinsic behaviour of framed structures.

Fox et al., (2014) conducted a comparative study of three existing capacity design methods for three existing methods of NZS3101, Priestley et al. (2007) and Pennucci et al. (2011). From the existing methods Pennucci et al. (2011) gave the best results and was subsequently used to develop a simplified method for determining the capacity design shear forces in coupled walls. Further the proposed method was then also verified through a case study application [10].

2.3 Review of Major International Codes

Some international codes suggest the expressions to prevent storey mechanism of collapse due to possible hinge formations in columns. This actually aims at attaining stronger columns with moment capacities more than those of beams framing into a particular joint considering safety margin.

American Standard: ACI 318M-2014 suggests that summation of moment capacities of column framing into a joint evaluated at the joint faces the minimum column moment considering factored axial loads along the direction of lateral forces resulting in, should be greater than or at least equal to 1.2 times the moment capacities of the beam framing into it [11].

$$\sum M_c \geq 1.2 \sum M_b \quad (2.2)$$

European Standard: EN1998-1:2003 recommends the relation between moment capacities of columns and moment capacity of beams for all joint can be written as,

$$\sum M_c \geq 1.3 \times \sum M_b \quad (2.3)$$

In this equation M_c is summation of the minimum moment capacities of the columns considering all design axial forces and M_b is summation of the moment capacities of the beams framing into the joint [12].

Zealand Standard: NZS3101:1995 documented the capacity design philosophy requirements considering over strength for beams that for the design of moment of resistance of columns, should be more than the moment of resistance of beams framing into a particular joint , New Zealand Standard recommends this aspect with respect to centre of the joint as follows:

$$\sum M_c \geq 1.4 \times \omega \sum M_b \quad (2.4)$$

In this equation ω is over strength factor for beams [13], [14].

Indian Standard: IS13920:1993 reported in view of some failure of joints and codal limitations, Jain et al., (2006) proposed a provision in draft for inclusion in IS13920:1993. According to that draft, at a joint, in a moment resisting frame which is designed for earthquake forces, the summation of the moment carrying capacities of the columns shall be at least equal to 1.1 times the summation of the moment carrying capacities of the beams along each individual joints in both direction [15].

Draft of IS13920:2014: At each beam-column joint of a moment-resisting frame, along each principal plane the sum of nominal design strength of columns meeting at that joint shall be at least 1.4 times of the sum of nominal design strength of beams meeting at individual joints in both direction. [16]

SAP2000 Documentation: Current seismic code (IS 13920:1993) does not cover beam-column flexural capacity ratio. However, as an interim arrangement, beam-column capacity ratio checks as outlined in the IS 13920 draft code have been adopted as described in this section. The program calculates the ratio of the sum of the beam moment capacities to the sum of the column moment capacities for ductile frames [17]. For Ductile frames, at a particular joint for a particular column direction, major or minor (IS 13920 Draft 7.2.1), the sum of moment capacities of columns and beams are related as,

$$\sum M_c \geq 1.1 \times \sum M_b \quad (2.5)$$

Where,

$\sum M_c$ = Sum of flexural strengths of columns framing into the joint, evaluated at the faces of the joint. Individual column flexural strength is calculated for the associated factored axial force.

$\sum M_b$ = Sum of flexural strengths of the beams framing into the joint, evaluated at the faces of the joint.

The beam-column capacity ratio is determined for a beam-column joint when the following conditions are met:

- a) the frame is ductile moment resisting
- b) a column of concrete material exists above the beam-column joint
- c) all of the beams framing into the column are concrete frame
- d) the connecting member design results are available
- e) the load combo involves seismic load

2.4 Review on Pushover Analysis

Pushover is a static-nonlinear analysis method where a structure is subjected to gravity loading and a monotonic displacement or force controlled lateral load pattern which continuously increases through elastic and inelastic behavior until an ultimate condition is reached. Due to some boundaries and difficulties of other methods push over analysis is considered as the most appropriate method as it requires less effort and deals with less amount of data for the analysis purpose for performance based seismic design .

A modified procedure was discussed by Bracci et.al. (1997) for pushover analysis. It consists of analysing the structure assuming triangular fixed lateral pushover load pattern [18]. This method is used to define the moment curvature relationship of the various members which is used as an input parameter and is utilized to capture the effect of local response. The effect of higher modes is neglected for the global response of structure.

A brief review done by Tso and Moghadam (1998) documented that the pushover analysis has been developed as a simplified procedure to provide information to the designers on the inelastic performance of buildings when subjected to earthquake excitation [19].

Rana et al., (2004) performed a case to observe the plastic rotations of the hinges formation of a 19-storey building in San Francisco by SAP2000, in order to check and find the performance limit suggested by FEMA and ATC guidelines [20].

Ho and Kwan (2008) concluded the flexural ductility of High Strength Concrete beams has been studied by an extensive parametric study based on pushover analysis taking into account the stress-path dependence of longitudinal steel reinforcement and confinement bars [21].

2.5 Previous Research on Seismic Risk Assessment

Recent developments in earthquake engineering, the seismic risk analysis has become more popular to ensure risk management in accordance with international building design codes and to provide an insight into the performances of building structures under seismic excitations. Development of seismic risk assessment for structures is experiencing radical variations generated by a variety of reasons. However, the current trend of procedure for seismic risk assessment of buildings structures requires identification of some steps (i) seismic hazard selection, (ii) analysis of structural fragilities, (iii) and calculation of performance limits. The structural fragility curves are said to be primary component while measuring the seismic risk assessment. Broadly, generation of fragility curves can be divided into three approaches namely (i) professional judgment, (ii) Empirical based (iii) Analytical based (Lupoi, 2005) [22].

Ellingwood (2001) highlighted the importance of the probabilistic analysis of building response for earthquake loading. The research outlined a relatively simple procedure for evaluating earthquake risk based on seismic fragility curve and seismic hazard curve [23].

Lagaros (2008) conducted fragility analyses of two groups of RC framed buildings. Four limit state fragility curves were developed on the basis of nonlinear static analysis and 95 % confidence intervals of the fragility curves were calculated. The case study concludes that the probability of exceedance of the significant damage state for the design earthquake (0.30g) [24].

Celik and Ellingwood (2010) studied the effects of uncertainties for input parameters. It was found that damping, concrete strength, and joint cracking have the greatest impact on the response statistics [25].

Rajeev and Tesfamariam (2012) demonstrated fragility based seismic vulnerability of buildings with consideration of soft storey and quality of construction on three, five, and nine storey Reinforced Concrete frames designed prior to 1970s [26]. Increasing the height of the columns of ground storey a soft ground storey was modelled analytically. Probabilistic seismic demand model (PSDM) for those buildings was developed, using the nonlinear finite element analysis.

Pragalath D. C. (2015) proposed on effective scheme of multiplication factor (MF) for design of OGS buildings that yields acceptable levels of reliability index [27].

A wide range of literature review in this area found, and majority of the literature presented work related to reliability analysis of building. There is no study effect of MCR on reliability.

2.6 Summary

This chapter discussed the MCR proposed by various literature and International code. Based on the study it was found that there is disparity exists in the values of MCR proposed by International Codes. There are guidelines given in the codes or any literature for the simplified calculation of MCR at a joint. It can be seen that the value of MCR is independent of the seismic zone. A review of various studies that uses pushover analysis, and fragility and reliability curves are discussed in the last part of this Chapter.

Chapter 3

Effect of MCR on the Seismic Performance of Buildings

3.1 Introduction

This chapter deals with effect of MCR on the seismic performance of building by pushover analysis. The plastic hinge formation of the beam column joints has studied by using commercial software SAP2000. Multiple steps of incremental displacement control methods are applied to find out the seismic performance of a six storey building designed as per IS 456. The overview of hinge formation pattern by pushover analysis is main focus of this chapter. Effect of values of MCR on the global and local failure on the building designed for Seismic zone V.

3.2 Pushover Analysis Procedure (FEMA 356)

FEMA 356:2000 describes the pushover analysis or non-linear static analysis procedure to estimate the seismic demand and capacity of the existing structure. In this procedure the magnitude of lateral load is increased monotonically along the height of the building [28]. The building is tried to displace up to the target displacement or until the collapse of the building. A curve, called pushover curve or capacity curve is drawn between base shear and roof displacement. Basically a hinge represents a localized force-displacement relation of a member through its elastic and inelastic phases under seismic loads. Typical one is as represented in Fig 3.1 , a flexural hinge represents the moment-rotation relation of a beam.

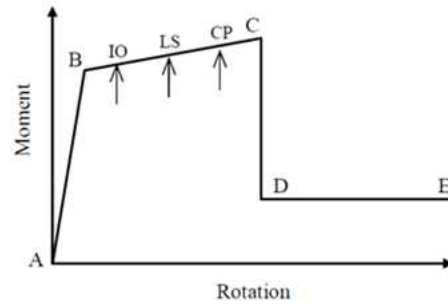


Figure 3.1: Typical Moment-Rotation curve showing performance levels

3.3 Selected Frames

Geometry of six storey building is considered and it is designed for two scenarios. In the first case, the MCR of all the beam column joint is kept below 1.2 (B1), and in the second case, the MCR of all the beam column joint is kept above 1.2 (B2). Storey height of 3.5 m is considered for the building with four bays having a uniform bay width of 5 m. Earthquake loads are calculated as per IS 1893: 2002 (Part-1) and the details of the parameters are given in Table 3.1 [29]. All the load combinations are considered as per the code. Dead load of the building includes self-weight of member, slab load (125mm thick) along with floor finish and wall load (15kN/m). Live load is considered to be $3\text{kN}/\text{m}^2$ in all floors. The RC design of the building frame is carried out as per IS 456:2002 and IS 13920: 1993 [15]. The nonlinear static (pushover) analysis of the two designed buildings are conducted as per the procedure outlined in Section 3.2. Fig. 3.2 present the sequence of hinge formation of the selected buildings (B1 and B2). It can be seen that when the building is designed with a MCR values above 1.2, the plastic hinges forms in beams. Whereas in the buildings with MCR values below 1.2, the plastic hinges form in columns in the initial steps itself that lead to failure of the entire building. The pushover curves of the two buildings are compared in Fig 3.3. The base shear capacity of the building B2 is found to be 75kN more than that of B1. The reduction in the base shear capacity of B1 may be attributed to the sequence of plastic hinges formations.

Table 3.1: Details of parameters considered for design

| | |
|---------------------------|--------|
| Seismic zone | IV |
| Soil type | Medium |
| Importance factor | 1 |
| Response reduction factor | 5 |
| Damping factor | 5% |

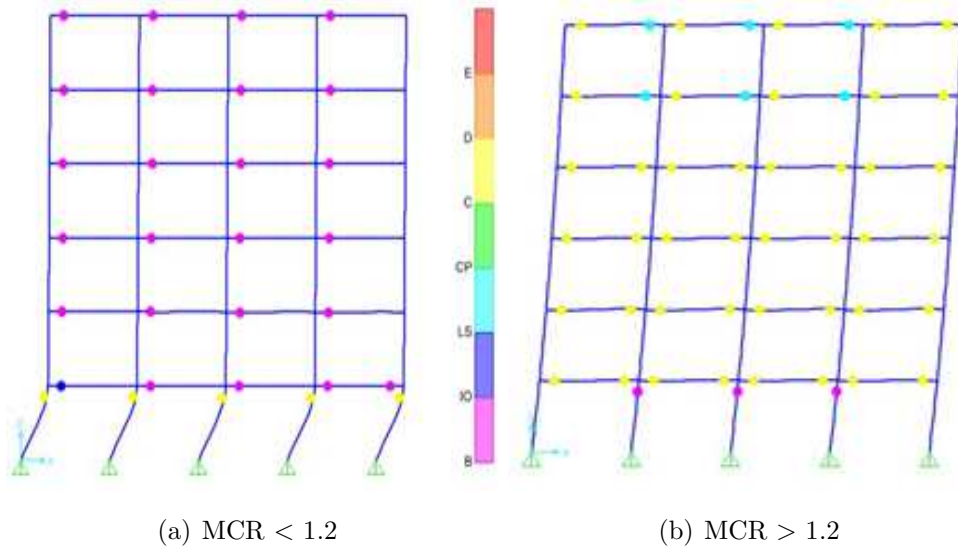


Figure 3.2: Global hinge status at 0.84 m displacement

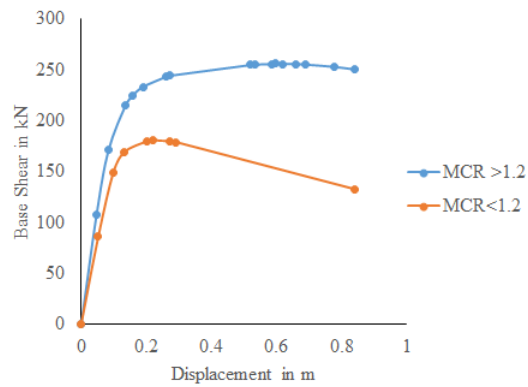


Figure 3.3: Comparison of pushover curve at 0.84 m displacement

3.4 Summary

This chapter defines Strong column and weak beam design philosophy clearly. This chapter discussed the effect of MCR on the seismic performance of building using pushover analysis. The MCR values is found to have significant effect on the seismic performance of frames. The sequence of formation of plastic hinges is greatly influenced by the MCR values.

Chapter 4

Development of Simplified Procedure for Estimating MCR

4.1 Introduction

The present chapter presents a procedure for calculation MCR by using SP16. In order to have more accurate calculation of MCR values, strength of material approach is used and a MATLAB program is developed to calculate the exact MCR value at the particular axial load in the column. This program uses the constitutive relation of concrete and steel as per Indian Standard IS 456:2000. The range of axial force in the most practical situations are found out to find out the minimum governing moment capacity of a column. Two methods are discussed in this chapter, one using SP-16 and another using analytical method. The minimum moment capacity required for the conservative estimation of MCR of a column is expressed in terms of the moment capacity of column at zero axial force.

4.2 Range of Normalized Axial Force in Buildings

Four code designed building models (4-storey, 6-storey, 8-storey, and 10-storey) are analysed with equivalent static approach to find out the axial force range for all the load combinations as per IS 1893 (2002) of various columns of the

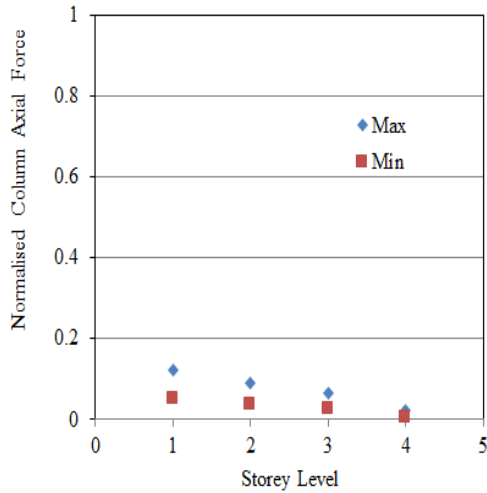
buildings [29]. All the design parameters are taken as same as that of the frames considered in Chapter-3. Table 4.1, 4.2, 4.3 and 4.4 shows the variation of axial force in each storeys in exterior and interior columns of four, six, eight and ten storeyed buildings respectively. P = maximum axial force carrying capacity of the column; P_{max} and P_{min} = maximum and minimum column axial force demand of the earthquake. The maximum and minimum axial loads in the columns are normalized with respect to the maximum axial load capacity of the column. The range of normalized axial load ratio of selected exterior and interior columns are also shown in the tables.

The variation of normalized axial forces in the selected exterior and interior columns in each storey are plotted graphically in Figs. 4.1-4.4 for four, six, eight and ten storeyed frames respectively.

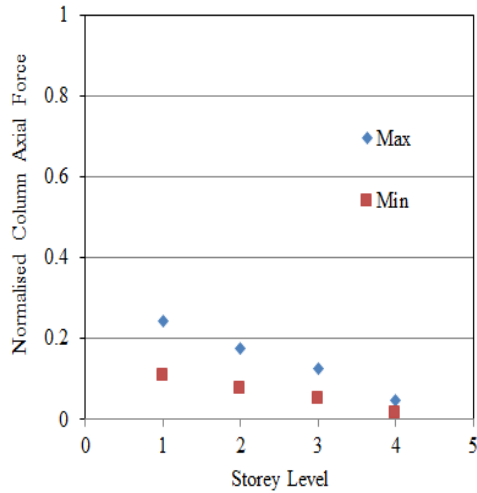
The Tables 4.1 to 4.4 and Figs. 4.1 to 4.4 show that range of normalized axial forces that generally the building columns experience is in the range of 0.1 to 0.4.(for interior column)

Table 4.1: Column axial force for four-storey building

| Storey Level | Exterior Column | | Interior Column | |
|--------------|----------------------|----------------------|----------------------|----------------------|
| | $\eta_1 = P_{max}/P$ | $\eta_2 = P_{min}/P$ | $\eta_1 = P_{max}/P$ | $\eta_2 = P_{min}/P$ |
| G | 0.124 | 0.052 | 0.245 | 0.109 |
| 1 | 0.089 | 0.036 | 0.176 | 0.077 |
| 2 | 0.064 | 0.025 | 0.127 | 0.053 |
| 3 | 0.023 | 0.006 | 0.046 | 0.015 |
| Mean | 0.06 | 0.025 | 0.151 | 0.065 |
| St. Dev. | 0.025 | 0.008 | 0.084 | 0.04 |



(a) Exterior Column

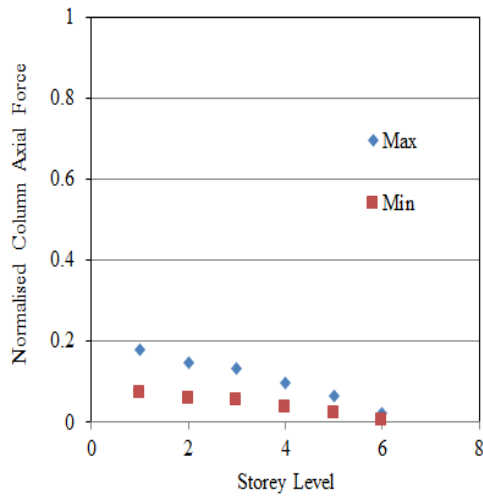


(b) Interior Column

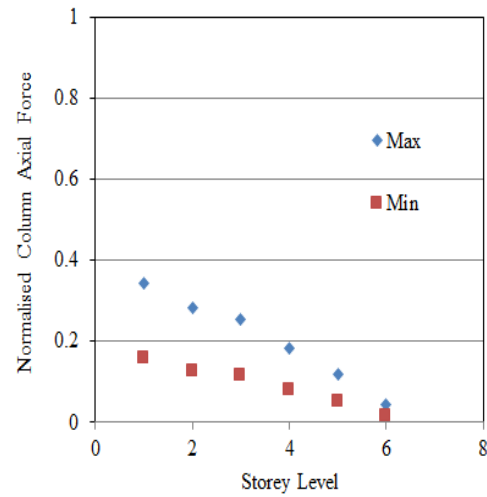
Figure 4.1: Column axial force for four-storey building.

Table 4.2: Column axial force for six-storey building

| Storey Level | Exterior Column | | Interior Column | |
|--------------|----------------------|----------------------|----------------------|----------------------|
| | $\eta_1 = P_{max}/P$ | $\eta_2 = P_{min}/P$ | $\eta_1 = P_{max}/P$ | $\eta_2 = P_{min}/P$ |
| G | 0.18 | 0.073 | 0.343 | 0.157 |
| 1 | 0.148 | 0.06 | 0.281 | 0.128 |
| 2 | 0.135 | 0.054 | 0.255 | 0.114 |
| 3 | 0.097 | 0.039 | 0.183 | 0.081 |
| 4 | 0.064 | 0.024 | 0.12 | 0.05 |
| 5 | 0.024 | 0.006 | 0.044 | 0.014 |
| Mean | 0.116 | 0.046 | 0.219 | 0.097 |
| St. Dev | 0.058 | 0.024 | 0.11 | 0.053 |



(a) Exterior Column

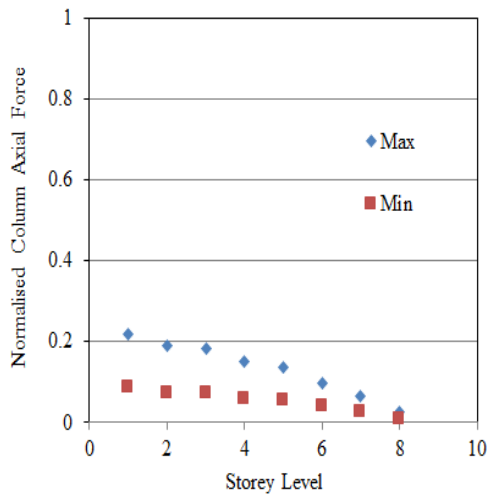


(b) Interior Column

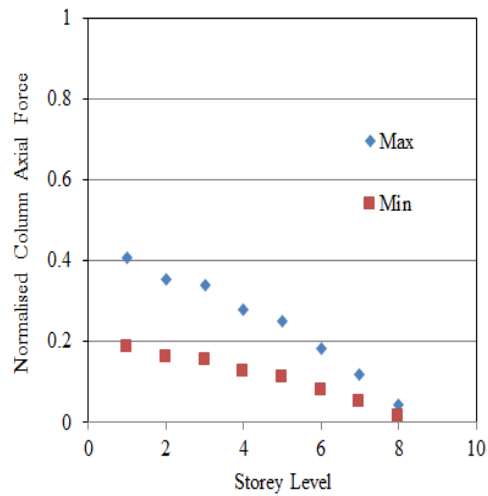
Figure 4.2: Column axial force for six-storey building.

Table 4.3: Column axial force for eight-storey building

| Storey Level | Exterior Column | | Interior Column | |
|--------------|----------------------|----------------------|----------------------|----------------------|
| | $\eta_1 = P_{max}/P$ | $\eta_2 = P_{min}/P$ | $\eta_1 = P_{max}/P$ | $\eta_2 = P_{min}/P$ |
| G | 0.218 | 0.085 | 0.407 | 0.187 |
| 1 | 0.19 | 0.074 | 0.352 | 0.162 |
| 2 | 0.183 | 0.072 | 0.339 | 0.155 |
| 3 | 0.151 | 0.06 | 0.278 | 0.126 |
| 4 | 0.137 | 0.054 | 0.251 | 0.113 |
| 5 | 0.099 | 0.039 | 0.181 | 0.079 |
| 6 | 0.066 | 0.025 | 0.12 | 0.05 |
| 7 | 0.025 | 0.007 | 0.044 | 0.014 |
| Mean | 0.144 | 0.057 | 0.265 | 0.119 |
| St. Dev | 0.066 | 0.027 | 0.124 | 0.059 |



(a) Exterior Column

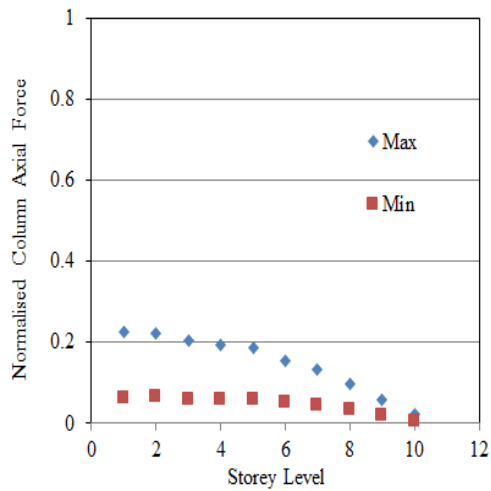


(b) Interior Column

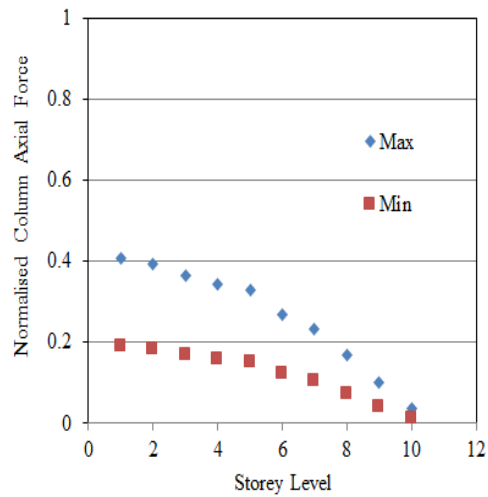
Figure 4.3: Column axial force for eight-storey building.

Table 4.4: Column axial force for Ten-storey building

| Storey Level | Exterior Column | | Interior Column | |
|--------------|----------------------|----------------------|----------------------|----------------------|
| | $\eta_1 = P_{max}/P$ | $\eta_2 = P_{min}/P$ | $\eta_1 = P_{max}/P$ | $\eta_2 = P_{min}/P$ |
| G | 0.227 | 0.062 | 0.407 | 0.189 |
| 1 | 0.222 | 0.067 | 0.395 | 0.183 |
| 2 | 0.204 | 0.059 | 0.363 | 0.169 |
| 3 | 0.193 | 0.06 | 0.342 | 0.158 |
| 4 | 0.186 | 0.06 | 0.328 | 0.15 |
| 5 | 0.153 | 0.051 | 0.269 | 0.122 |
| 6 | 0.133 | 0.045 | 0.232 | 0.104 |
| 7 | 0.096 | 0.034 | 0.167 | 0.073 |
| 8 | 0.06 | 0.02 | 0.102 | 0.042 |
| 9 | 0.023 | 0.005 | 0.038 | 0.011 |
| Mean | 0.17 | 0.055 | 0.298 | 0.136 |
| St. Dev | 0.07 | 0.02 | 0.127 | 0.061 |



(a) Exterior Column



(b) Interior Column

Figure 4.4: Column axial force for ten-storey building.

4.3 MCR Using the Design Charts of SP-16

In order to investigate what moment capacity a column may pose under these ranges of axial force, respective column interaction diagrams given in SP-16 (1980) are superposed with the obtained axial force range and presented in Fig. 4.5 [30]. The results are summarized in Table 4.5. In order to obtain the range of moment capacities corresponding to the range of normalized axial forces in a column section, a typical column section from design charts of SP-16 (1980) is considered. Fig. 4.5 shows the axial force versus moment interaction curve of a typical column section from SP-16 and the range of axial loads (0.1 to 0.4) obtained from the analysis is indicated in the plot to obtain the corresponding range of moment capacities for interior column and 0.06 to 0.23 for exterior column. In most of the situations, the maximum moment carrying capacity of the column may lie within the range of axial loads in the 0.1 to 0.4 for interior and 0.06 to 0.23 for exterior column. The minimum moment capacity in most of the cases corresponds to the moment capacity at normalized axial force ratio of 0.4 for exterior and 0.23 for interior column. In order to obtain the minimum moment capacity for the calculation of the MCR, the maximum and minimum moment capacities are calculated for various columns as shown in Table 4.5. In some situations due to the nature of moment versus axial load interaction curve, the minimum value of moment capacity may be governed by maximum axial force. The minimum moment capacity ratio, which is the ratio of minimum moment capacity to the moment capacity at zero axial load, is calculated for selected exterior and interior columns as shown in Fig. 4.5. This minimum value of this is obtained as 0.8, which means that the minimum moment capacity of the column can be taken conservatively as 0.8 times the moment capacity at zero axial force.

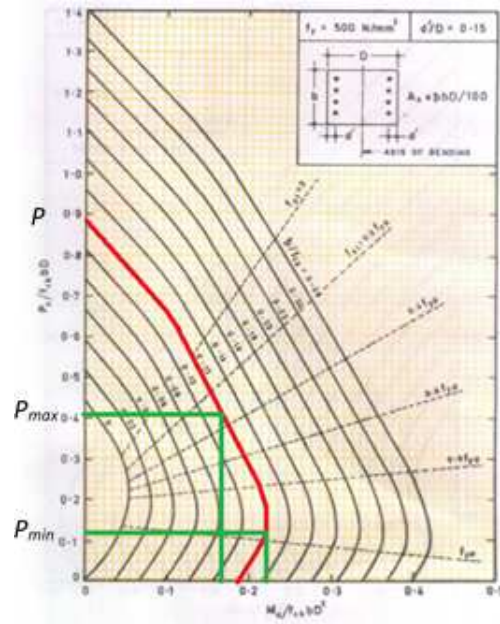


Figure 4.5: Column axial force range (typical) for interior column shown in design chart of SP 16

Table 4.5: Column Moment Capacities

| Col. ID | $\frac{P_{max}}{f_{ck}bD}$ | $\frac{M(P_{max})}{f_{ck}bD^2}$ | $\frac{P_{min}}{f_{ck}bD}$ | $\frac{M(P_{min})}{f_{ck}bD^2}$ | $\frac{M_{min}}{f_{ck}bD^2}$ | $\frac{M_{P=0}}{f_{ck}bD^2}$ | $\frac{M_{min}}{M_{P=0}}$ |
|---------|----------------------------|---------------------------------|----------------------------|---------------------------------|------------------------------|------------------------------|---------------------------|
| 4CE | 0.21 | 0.22 | 0.08 | 0.22 | 0.22 | 0.24 | 0.92 |
| 4CI | 0.42 | 0.23 | 0.19 | 0.26 | 0.23 | 0.26 | 0.89 |
| 6CE | 0.26 | 0.18 | 0.10 | 0.19 | 0.18 | 0.18 | 1.00 |
| 6CI | 0.50 | 0.13 | 0.22 | 0.17 | 0.13 | 0.15 | 0.87 |
| 8CE | 0.27 | 0.18 | 0.11 | 0.19 | 0.18 | 0.18 | 1.00 |
| 8CI | 0.51 | 0.14 | 0.23 | 0.17 | 0.14 | 0.17 | 0.82 |
| 10CE | 0.30 | 0.13 | 0.08 | 0.16 | 0.13 | 0.13 | 1.00 |
| 10CI | 0.52 | 0.12 | 0.25 | 0.16 | 0.12 | 0.15 | 0.80 |

4.4 Minimum Moment Capacity Analytical Method

Strain compatibility is most important for determining the stresses in concrete and steel, and hence, their respective resultant forces in concrete (P_c) and same in steel (P_s) can be determined. Applying the condition of static equilibrium, it follows that the two design strength components are easily obtainable as:

$$P_{uR} = P_c + P_s \quad (4.1)$$

$$M_{uR} = M_c + M_s \quad (4.2)$$

Where, M_c and M_s denote the resultant moments due to P_c and P_s respectively, with respect to the centroidal axis. From the nature of the equilibrium equations (Eq. 4.1 and 4.2) it may be observed that, for a given location of the neutral axis ($\frac{x_u}{D}$), the design strength values P_{uR} and M_{uR} can be directly determined. However, given an arbitrary value of eccentricity (e), it is possible to arrive at the design strength (P_{uR} or $M_{uR} = P_{uR} \times e$) using Eq. 4.1, only after first locating the neutral axis, which can be achieved by considering moments of forces P_c and P_s about the eccentric line of action of P_{uR} , and applying static equilibrium. Unfortunately, the expressions for P_c and P_s in terms of x_u are such that, in general, it will not be possible to obtain a closed-form solution for x_u in terms of e . The relationship is highly nonlinear, requiring a trial-and-error solution. The interaction curve defines the different (M_{uR} , P_{uR}) combinations for all possible eccentricities of loading $0 \leq e < \infty$. For design purposes, the calculations of M_{uR} and P_{uR} are based on the design stress-strain curves including the partial safety factors (Pillai and Menon, 2015) [31].

Generalized expressions of the resultant force in the concrete (P_c) as well as its moment (M_c) with respect to the centroidal axis of bending may be derived as follows, based on Fig. 4.6:

$$P_c = a \times f_{ck} \times b \times D \quad (4.3)$$

$$a = \begin{cases} 0.362 \times \frac{x_u}{D}, & \text{for } x_u \leq D \\ 0.447 \times \left(1 - \frac{4g}{21}\right), & \text{for } x_u > D \end{cases} \quad (4.4)$$

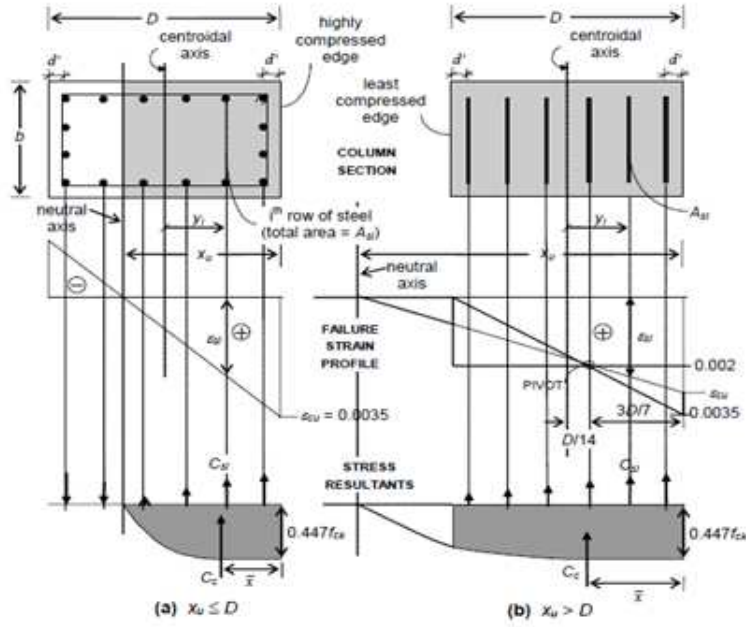


Figure 4.6: Analysis of design strength of a rectangular section under eccentric compression (a) neutral axis within the section, (b) neutral axis outside of the section (Pillai and Menon, 2015)

$$M_c = P_c \left(\frac{D}{2} - \bar{x} \right) \quad (4.5)$$

Where, a = stress block area factor, \bar{x} = distance between highly compressed edge and the line of action of P_c (i.e., centroid of stress block area)

$$\bar{x} = \begin{cases} 0.416 \times x_u, & \text{for } x_u \leq D \\ \left(0.5 - \frac{8g}{49} \right) \times \left(\frac{D}{\left(1 - \frac{4g}{21} \right)} \right), & \text{for } x_u > D \end{cases} \quad (4.6)$$

Similarly, the expressions of the resultant force in the steel (P_s) as well as its moment (M_s) with respect to the centroidal axis of bending is easily obtained as:

$$P_s = \sum_{i=1}^n (f_{si} - f_{ci}) \times A_{si} \quad (4.7)$$

$$M_s = \sum_{i=1}^n (f_{si} - f_{ci}) \times A_{si} \times y_{si} \quad (4.8)$$

Where, A_{si} = area of steel in the i th row (of n rows) y_i = distance of i th row of steel from the centroidal axis, measured positive in the direction towards the highly compressed edge; f_{si} = design stress in the i th row (corresponding to the strain ε_{si}) obtainable from design stress-strain curves for steel; ε_{si} strain in the i th row, obtainable from strain compatibility conditions (ε_{si} and f_{si} are assumed to be positive if compressive, and negative if tensile); f_{ci} design compressive stress level in concrete, corresponding to the strain $\varepsilon_{ci} = \varepsilon_{si}$ adjoining the i th row of steel, can be obtained from the design stress-strain curve for concrete [Note: $f_{ci} = 0$ if the strain is tensile]:

$$f_{ci} = \begin{cases} 0, & \text{for } \varepsilon_{si} \leq 0 \\ 0.447 \times f_{ck}, & \text{for } \varepsilon_{si} \geq 0 \\ 0.447 \times f_{ck} \left[2 \left(\frac{\varepsilon_{si}}{0.002} \right) - \left(\frac{\varepsilon_{si}}{0.002} \right)^2 \right] & \text{otherwise} \end{cases} \quad (4.9)$$

Also, from Fig. 4.6, it can be observed (applying similar triangles) that:

$$\varepsilon_{si} = \begin{cases} 0.0035 \times \frac{\left[x_u - \frac{D}{2} + y_i \right]}{x_u}, & \text{for } x_u \leq 0 \\ 0.0035 \times \frac{\left[1 + \frac{y_i - \frac{D}{2}}{\frac{3D}{7}} \right]}{x_u - \frac{7}{D}}, & \text{for } x_u > 0 \end{cases} \quad (4.10)$$

The formulation, governing equation for the component (M_c , M_s , P_c , P_s), stress- strain profile etc are taken from Indian standard design codes. (SP 16:1980, Pillai and Menon, 2015, and IS 456:2000). A MATLAB (MatLab, 2015) program is written based on the above sectional equilibrium approach to plot the P-M interaction curve [32]. The moment capacities obtained for the selected sections are compared with the values in Pillai and Menon, (2015) as shown in Table 4.6. The results show that the program is found to be validated.

Table 4.6: Validation of computer programs with Pillai and Menon, 2015

| $\frac{x_u}{D}$ | P_{uR} (kN) Computer Program | P_{uR} (kN) Pillai and Menon | M_{uR} (kN – m) Computer Program | M_{uR} (kN – m) Pillai and Menon |
|-----------------|-----------------------------------|-----------------------------------|---------------------------------------|---------------------------------------|
| 0.30 | 33.1 | 33 | 203 | 203.1 |
| 0.34 | 125.1 | 125 | 210.5 | 210.6 |
| 0.38 | 269.2 | 268.6 | 216.9 | 216.9 |
| 0.42 | 412.6 | 412.2 | 222 | 222 |
| 0.46 | 545.5 | 545.3 | 225 | 225.1 |
| 0.50 | 667.8 | 667.8 | 226.9 | 226.9 |
| 0.54 | 777.4 | 785.9 | 226.4 | 226.4 |
| 0.58 | 893.9 | 900.5 | 224.3 | 224.4 |
| 0.62 | 1013.1 | 1018.3 | 219.4 | 219.5 |
| 0.66 | 1158.8 | 1162.4 | 207.7 | 207.9 |
| 0.70 | 1295.5 | 1298.3 | 196.1 | 196.2 |
| 0.74 | 1423.2 | 1425.6 | 184.6 | 184.7 |
| 0.78 | 1543.5 | 1545.5 | 173.1 | 173.2 |
| 0.82 | 1657.2 | 1659 | 161.5 | 161.6 |
| 0.86 | 1763.6 | 1764.5 | 149.7 | 149.7 |
| 0.9 | 1846.7 | 1857.6 | 139.6 | 137.7 |
| 0.94 | 1937.2 | 1946.5 | 127 | 125.3 |
| 0.98 | 2022.6 | 2030.5 | 113.9 | 112.5 |
| 1.02 | 2094.1 | 2102.6 | 101.3 | 100.2 |
| 1.06 | 2157.3 | 2157.7 | 90.2 | 90.1 |
| 1.10 | 2211.8 | 2204.4 | 80.9 | 81.5 |
| 1.14 | 2256 | 2244.2 | 73.5 | 74.2 |
| 1.18 | 2298.4 | 2278.6 | 66.3 | 67.9 |
| 1.22 | 2335.8 | 2308.6 | 59.8 | 62.4 |
| 1.26 | 2368.3 | 2334.5 | 54.1 | 57.5 |
| 1.3 | 2399.6 | 2357.2 | 48.5 | 53.1 |

4.5 Minimum Moment Capacity Column - SP16 v/s Analytical Method

Two blocks of an existing building hospital building (as shown in Fig. 4.7) in Jamshedpur, India are considered. Figs. 4.7a and 4.7b show the three dimensional and plan view of Block D and Figs. 4.8a and 4.8b show the three dimensional and plan view of Block A respectively. An equivalent static analysis is conducted to obtain the axial force ranges in arbitrarily selected column sections. The moment capacities for minimum and maximum axial forces are calculated to find out the governing minimum moment capacities in all the columns. Table 4.7 and 4.8 show the calculated values of minimum moment ratio $\frac{M_{min}}{M_{p=0}}$ for all the columns in block-D and block-A respectively using both for SP-16 method and Analytical method.

The factor, $\frac{M_{min}}{M_{p=0}}$ obtained using SP-16 and analytical method are found to be in the range of 0.84 to 1.08 (from Table 4.7 and 4.8). Therefore an Equation can be proposed to calculate the column moment capacity, M_c in terms of moment capacity at zero axial force $M_{c,P=0}$ can be proposed as.

$$\sum M_c = 0.8 \times \sum M_{c,P=0} \quad (4.11)$$

Table 4.7: Result of existing building Block-D

| Col Id | Size (BD) (mmmm) | Reinforcement | P_{max} (kN) | P_{min} (kN) | $\frac{M_{min}}{M_{p=0}}$ (Matlab Program) | $\frac{M_{min}}{M_{p=0}}$ (by SP16) | Variation in % |
|--------|------------------------|-----------------|-------------------|-------------------|--|--|-------------------|
| C-1 | 230×400 | 8 NOS 16 ϕ | 393.4 | 40.5 | 0.91 | 1.01 | 9.9 |
| C-2 | 230×400 | 8 NOS 16 ϕ | 647.7 | 16.9 | 0.92 | 1.00 | 8.0 |
| C-3 | 230×400 | 8 NOS 16 ϕ | 573.6 | 11.3 | 0.93 | 1.00 | 7.0 |
| C-4 | 230×400 | 8 NOS 16 ϕ | 353.9 | 35.0 | 0.91 | 1.01 | 9.9 |

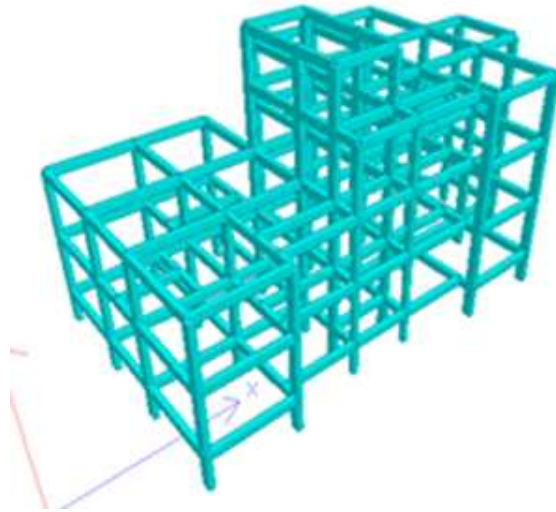


Figure 4.7: 3D view of Block-D, staff quarter Jamshedpur (G+2)

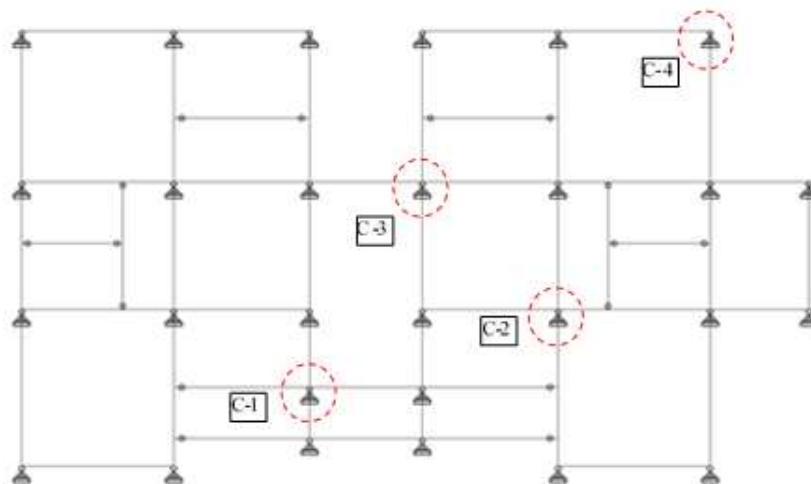


Figure 4.8: Plan view of Block-D, staff quarter Jamshedpur (G+2)

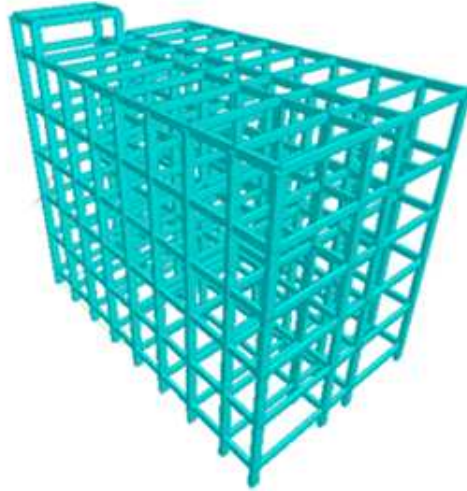


Figure 4.9: 3D view of Block-A, Jamshedpur Hospital Building (G+4)

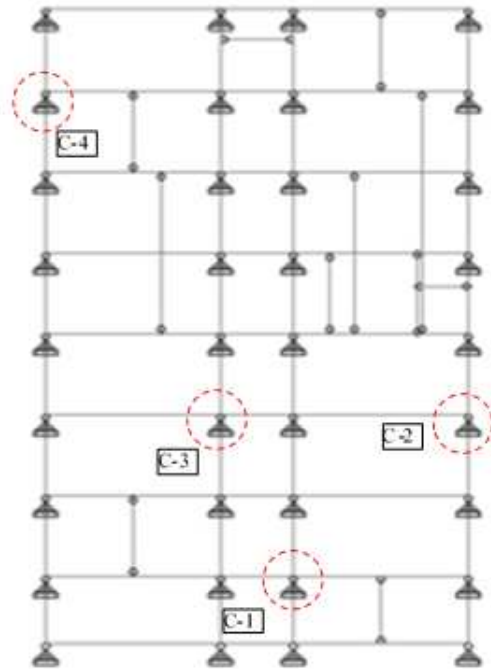


Figure 4.10: Plan view of Block-A, Jamshedpur Hospital Building (G+4)

Table 4.8: Result of existing building Block-A

| Col Id | Size (BD) (mmmm) | Reinforcement | P_{max} (kN) | P_{min} (kN) | $\frac{M_{min}}{Mp = 0}$ (Matlab Program) | $\frac{M_{min}}{Mp = 0}$ (by SP16) | Variation in % |
|--------|------------------------|-----------------|-------------------|-------------------|---|---------------------------------------|-------------------|
| C-1 | 300×600 | 8 NOS 16 ϕ | 1339.2 | 95.3 | 0.85 | 1.01 | 15.8 |
| C-2 | 300×600 | 8 NOS 16 ϕ | 1414 | 56.9 | 0.86 | 1 | 14 |
| C-3 | 300×600 | 8 NOS 16 ϕ | 1580.2 | 146.7 | 0.92 | 1.02 | 9.8 |
| C-4 | 300×600 | 8 NOS 16 ϕ | 1784.5 | 70.7 | 1.08 | 1.01 | 6.9 |

4.6 Summary

The range of axial force in the typical building frames ranging from four to ten storey are found out. The range of axial force is found to be 0.1–0.4 for exterior column and 0.06–0.23 for interior column. Two methods are discussed in this chapter, one using SP-16 and another using analytical method. The values of minimum moment capacity for an existing building is calculated by both methods. The minimum moment carrying capacity can be conservatively determined to be about 0.8 times the moment capacity at zero axial force in a column.

Chapter 5

Effect of MCR on Fragility and Reliability

5.1 General

This chapter of the thesis deals with the fragility and reliability analysis of four storey RC frames designed using various values of MCR ranging from 1.0 to 3.2 (ref APPENDIX-B for section details). The RC frames are designed as per IS 1893 (2002) for all seismic zones. Hazard curves required of various seismic location in India (like zone II, III, IV and V) has been selected from National Disaster Management Authority, Government of India [33]. Seismic risk assessment of all the designed buildings is conducted and based on the achieved Reliability Index and the Target Reliability Index minimum value of MCR is suggested.

5.2 Earthquake Risk Assessment

Ellingwood (2001) reported the methodology for estimation of seismic risk which includes three steps. First part is the identification of the seismic hazard of a location, $P[A = a]$, described by the annual probability of occurrence of specific levels of earthquake motion [23]. The seismic hazard at a site is usually represented through a hazard curve, $GA(x)$ which is a plot of $P[A = a]$ versus the level peak earthquake acceleration (a) expressed in terms of gravitational acceleration (g). Second part is global response analysis of the structural system subjected to

earthquake motions.

$$P[LS_i] = \sum_a P[LS_i|A = a]P[A = a] \quad (5.1)$$

The response analyses of the structure is carried out by conducting nonlinear time history analyses for different earthquakes, and the response is expressed in terms of maximum inter-storey drift at any storey. Third part is calculation of limit state probabilities of attaining a series of limit states, LS_i , through the Eq. (5.1).

The conditional probability, $P[LS_i|A = a]$ in eqn. 5.2 is defined as the seismic fragility, $FR(x)$. This is the probability of meeting or exceeding a specified level of damage, LS , given a ground motion which has a certain level of intensity. This conditional probability is often assumed to follow lognormal probability distribution parameter (Cornell et. al, 2002; Song and Ellingwood, 1999) [34]. A point estimate of the limit state probability of state i can be obtained by convolving the fragility $FR(x)$ with the derivative of the seismic hazard curve, $GA(x)$, thus removing the conditioning on acceleration as per Eq. (5.2).

$$P[LS_i] = \int FR(x) \frac{dGA}{dx} dx \quad (5.2)$$

The parameters of the fragility-hazard interface must be dimensionally consistent for the probability estimate to be meaningful.

Reliability Index, that gives the measurement of safety margin, is used in the present study to assess the performance of various buildings with varying MCR. Reliability Index corresponding to the probability of failure can be found by the following standard equation as shown below:

$$\beta_{Pf} = -\phi^{-1}(P[LS_i]) \quad (5.3)$$

Where, $\phi()$ represents the standard normal distribution.

Therefore the methodology of the present chapter can be summarized as to develop a seismic hazard curve for the selected region using probabilistic seismic hazard analysis and fragility curves for the selected buildings and to arrive at the probability of failure (Eq. 5.2) and associated reliability index (Eq. 5.3) for different limit states. The next two sections represents the methods of developing seismic hazard curve and fragility curve.

5.2.1 Seismic Hazard Curves

Present study uses seismic hazard curves developed by National Disaster Management Agency, Govt. of India, for the reliability analysis [33]. The seismic hazard curves having maximum probability of occurrence in a particular seismic zone is selected (ref. APPENDIX-A). Fig 5.1 shows the selected seismic hazard curves for seismic zones II, III, IV and V. The PGA values at 50%, 10% and 2% probabilities of occurrence for each zone are plotted in Fig 5.1 and tabulated in Table 5.1. These values are used for the calculation of reliability index for the specific performance objectives.

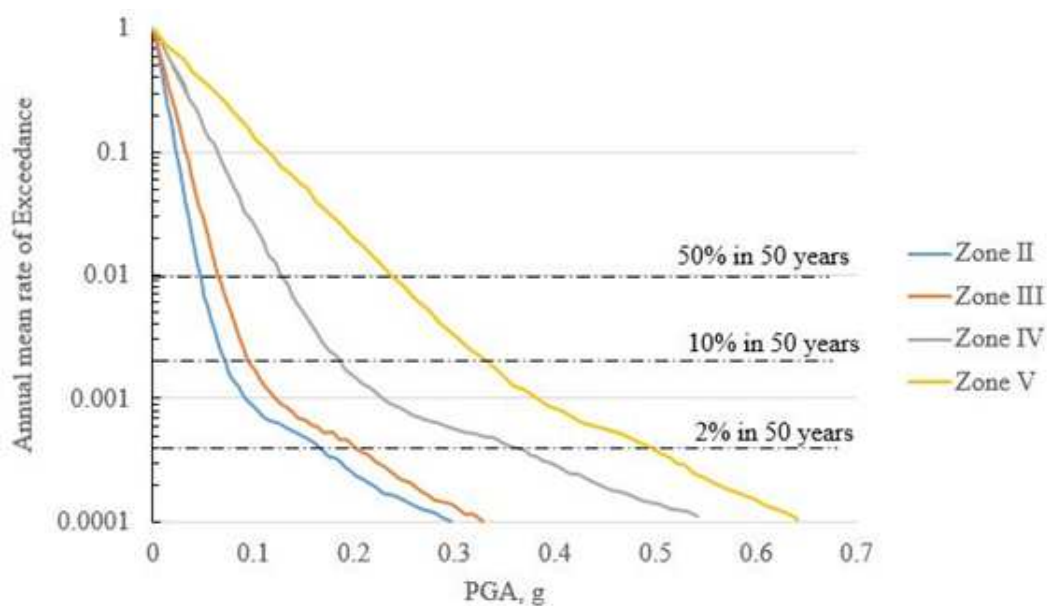


Figure 5.1: Different Hazard level at the selected location (<http://www.ndma.gov.in/en/>)

5.2.2 Development of Fragility Curves

The fragility function represents the probability of exceedance of a selected Engineering Demand Parameter (EDP) for a selected structural limit state (LS) for a specific ground motion intensity measure (IM). The seismic fragility, $FR(x)$ can be expressed in closed form using the following equation,

Table 5.1: Different Hazard level at selected location

| Location | PGA (g) at Probability of Occurrence of 50% in 50 years | PGA (g) at Probability of Occurrence of 10% in 50 years | PGA (g) at Probability of Occurrence of 2% in 50 years |
|----------|--|--|---|
| Zone II | 0.045 | 0.072 | 0.17 |
| Zone III | 0.065 | 0.085 | 0.20 |
| Zone IV | 0.125 | 0.18 | 0.35 |
| Zone V | 0.23 | 0.33 | 0.51 |

$$P(D \geq |IM) = 1 - \phi \left(\frac{\ln \frac{S_C}{S_D}}{\sqrt{\beta_{D|IM}^2 + \beta_C^2 + \beta_M^2}} \right) \quad (5.4)$$

Where, D is the drift demand, C is the drift capacity at chosen limit state, S_C and S_D are the chosen limit state and the median of the demand (LS) respectively. $\beta_{d|IM}$, β_C and β_M are dispersions of the intensity measure, capacities and modelling respectively. A fragility curve can be obtained for different limit states using Eq. 5.4.

Probabilistic Seismic Demand Model (PSDM)

The seismic demand (SD) is usually described through probabilistic seismic demand models (PSDMs) particularly for nonlinear time history analyses (NLTH) which are given in terms of an intensity measure (IM). It has been suggested by Cornell et. al. (2002) that the estimate of the median demand, EDP (SD) can be represented in a generalized form by a power model as given in Eq. 5.5 [34].

$$EDP = a(IM)^b \quad (5.5)$$

Where, a and b are the regression coefficients of the PSDM. Eq. 5.5 can be rewritten for system fragilities as follows:

$$P(D \geq |IM) = 1 - \phi \left(\frac{\ln(S_C) - \ln(a \cdot IM^b)}{\sqrt{\beta_{D|IM}^2 + \beta_C^2 + \beta_M^2}} \right) \quad (5.6)$$

The dispersion, $\beta_{d|IM}$, of inter-storey drifts from the time history analysis can be calculated using Eq. 5.6 where $a(IM)^b$ represents the mean inter-storey drift.

$$\beta_{d|IM} = \sqrt{\frac{\sum [\ln(d_i) - \ln(a \cdot IM^b)]^2}{N - 2}} \quad (5.7)$$

Uncertainty associated with building definition and construction quality (β_c) accounts for the possibility that the actual properties of structural elements. ATC 58 (2012) recommends values for β_c under representative conditions and for this study β_c has taken as 0.25 [35].

According to ATC 58 (2012), modelling uncertainty (β_m) is the result from inaccuracies in component modelling, damping and mass assumptions. For the purpose of estimating m, this uncertainty has been associated with the dispersion of building definition and construction quality assurance (β_c) and the quality and completeness of the nonlinear analysis model (β_q). The total modelling dispersion can be estimated as follows:

$$\beta_m = \sqrt{\beta_c^2 + \beta_q^2} \quad (5.8)$$

In this study β_q is assumed to be 0.25.

In order to withstand different levels of damage Limit states define the capacity of the structure. The median inter-storey drift limit states for RC moment resisting frame structures defining the capacity of the structure at various performance levels (S_C) are suggested in published literature. The median inter-storey drifts for various performance limits are listed in Table 5.2 considered in the present study.

Table 5.2: Damage limits and dispersion associated with various structural performance levels

| Limit states | Performance levels | Median Inter-storey Drifts S_c | Dispersion, β_c |
|--------------|----------------------------|----------------------------------|-----------------------|
| IO | Light repairable damage | 1 | 0.25 |
| SD | Moderate repairable damage | 2 | 0.25 |
| CP | Near collapse | 4 | 0.25 |

5.3 Sampling of Variables

In structural engineering analysis, material properties like strength and stiffness, structural properties like damping ratio are random in nature. These properties depend on various parameters like type of construction, quality of construction, etc. To represent these parameters by considering mean value is not correct for each time; hence proper sampling is required in order to estimate the most accurate results. To estimate the characteristics of the whole population, a subset of individuals within the population are selected which is normally known as sampling. McKay et al. (1979) proposed an attractive alternative method in computer experiments called as Latin Hypercube Sampling (LHS) [36]. Table 5.3 represents the details of random variable used in LHS.

Table 5.3: Details of random variables used in LHS scheme

| Material/ Property | Variable | Mean | COV (%) | Distribution | Remarks |
|-----------------------|----------|------------|------------|--------------|--------------|
| Concrete | fck | 30.28 MPa | 21 | Normal | Uncorrelated |
| Steel | fy | 468.90 MPa | 10 | Normal | Uncorrelated |
| Damping ratio | ξ | 5% | 40 | Normal | Uncorrelated |

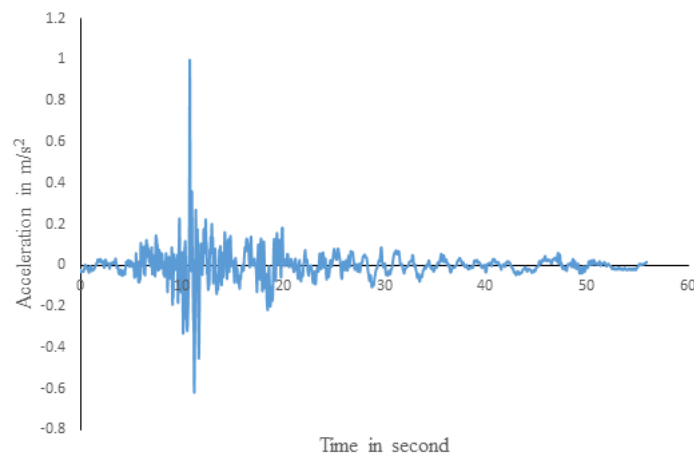


Figure 5.2: Time history data (<http://strongmotioncenter.org/>)

5.4 Probabilistic Seismic Demand Models

Probabilistic seismic demand models (PSDMs) direct the Engineering Damage Parameter (EDP) in order to express a function of Intensity Measure (Cornell et al., 2002) [34]. The standard seismic hazard curves from various seismic location has taken in terms of PGA. Hence, the PGA is selected as the intensity measure in this study.

Nonlinear time history analysis is done for all the selected building models by Opensees to find out the inter-storey drift [37]. For each floor the maximum inter-storey drift is plotted with PGA in a normal scale. In order to obtain the constant a, and b of the power law model of best fit curve plotted. Fig. 5.3 represents PSDM model for the selected buildings under given earthquake considered. From this plot it is clear that with the increment of MCR corresponding drift % is decreasing.

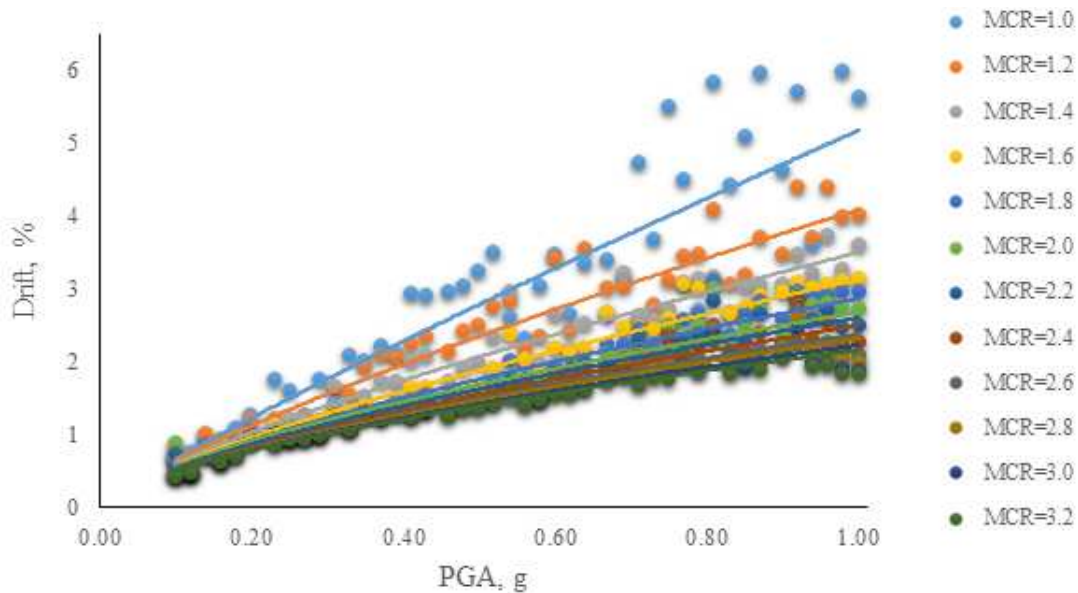


Figure 5.3: PSDM model for the selected buildings under given earthquake

5.5 Fragility Curves

Once PSDM models and the dispersions ($\beta_{D|PGA}$, β_c , and β_m) for all the frame models are calculated, the second part, fragility curves for various performance

levels are developed using the Eq. 5.4 for different performance levels. Fragility curves for all the MCR (1.0-3.2) in each frame are evaluated.

Figs. 5.4, 5.5 and 5.6 represents the fragility curve of the selected building for performance limits IO, SD and CP respectively. Fragility analysis show that as the MCR value increases the probability of exceedance decreases proportionately.

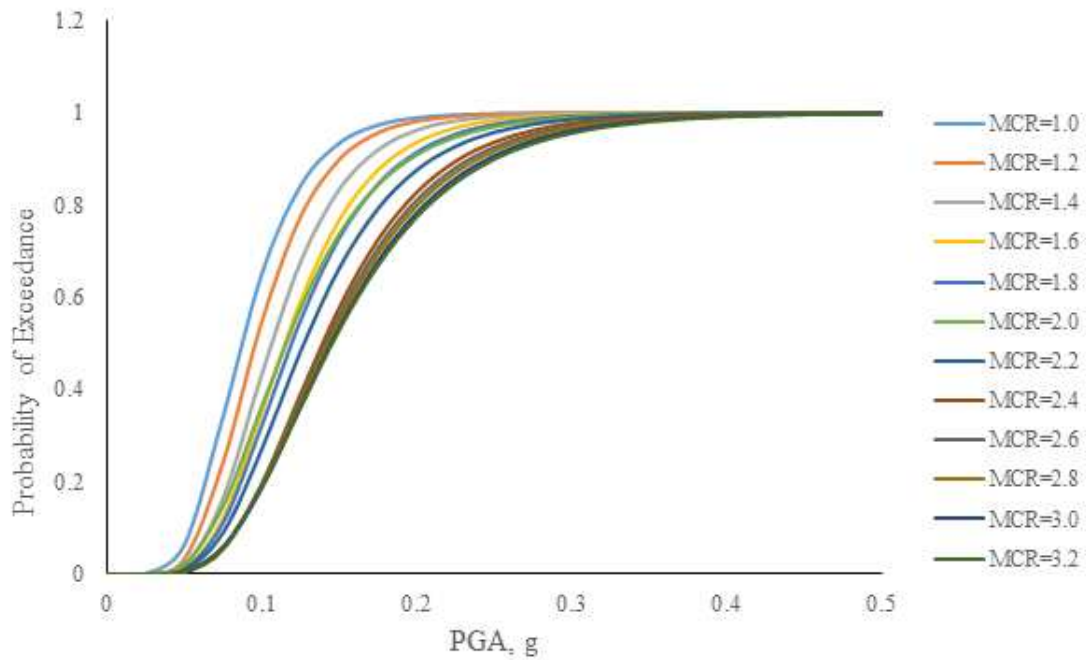


Figure 5.4: Fragility curve of IO for various MCR

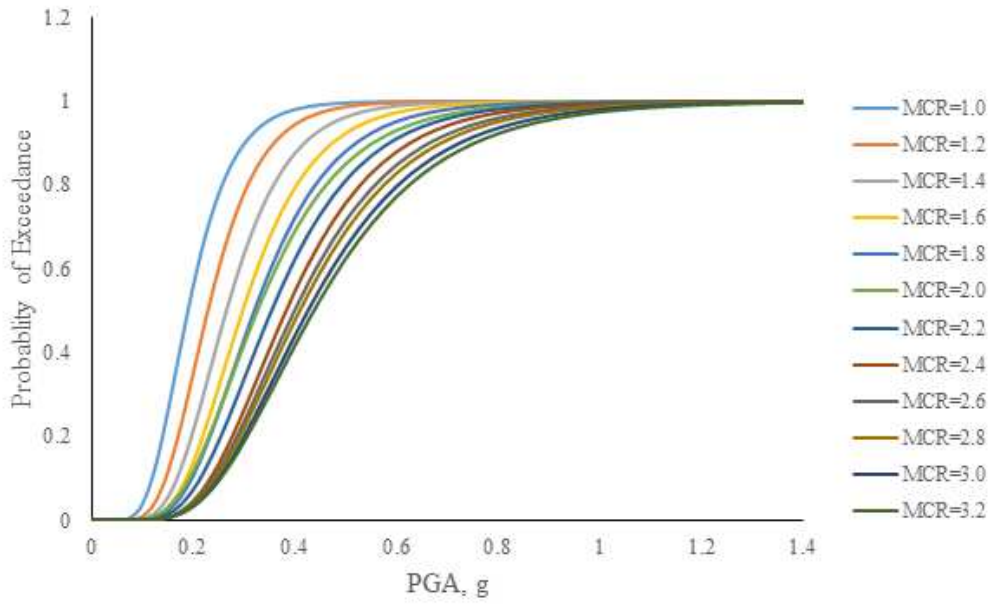


Figure 5.5: Fragility curve of SD for various MCR

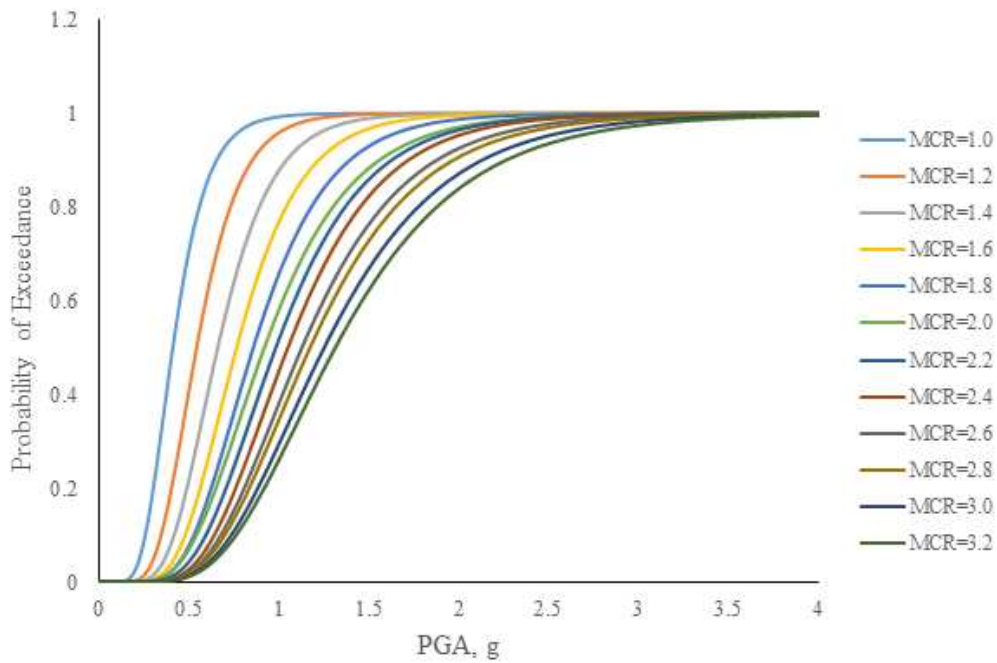


Figure 5.6: Fragility curve of CP for various MCR

5.6 Reliability Curves

Reliability indices are calculated for all the previously selected buildings for different performance objectives using Eq. 5.3 through a numerical integration. The fragility curve, $FR(x)$ and seismic hazard curve $GA(x)$ are combined to evaluate the limit state probability, $P[LS_i]$ and the corresponding reliability index, β_{Pf} . Reliability curve is obtained by the discussed formulation from fragility curve. Fig. 5.7 presents a typical Reliability curve of CP for Seismic Zone II for the selected buildings. Reliability index of a building depends on MCR values. As the MCR increases the reliability also increases. Table 5.4, 5.5 and 5.6 represents the Target Reliability for IO, SD and CP respectively for various hazard location. In order to obtain an estimate of minimum value of MCR required in a building, the achieved values of reliability is compared with the target values of reliability indices (tabulated in Table 5.7). As the seismic zone increases the MCR value also shall be increased to achieve a target reliability.

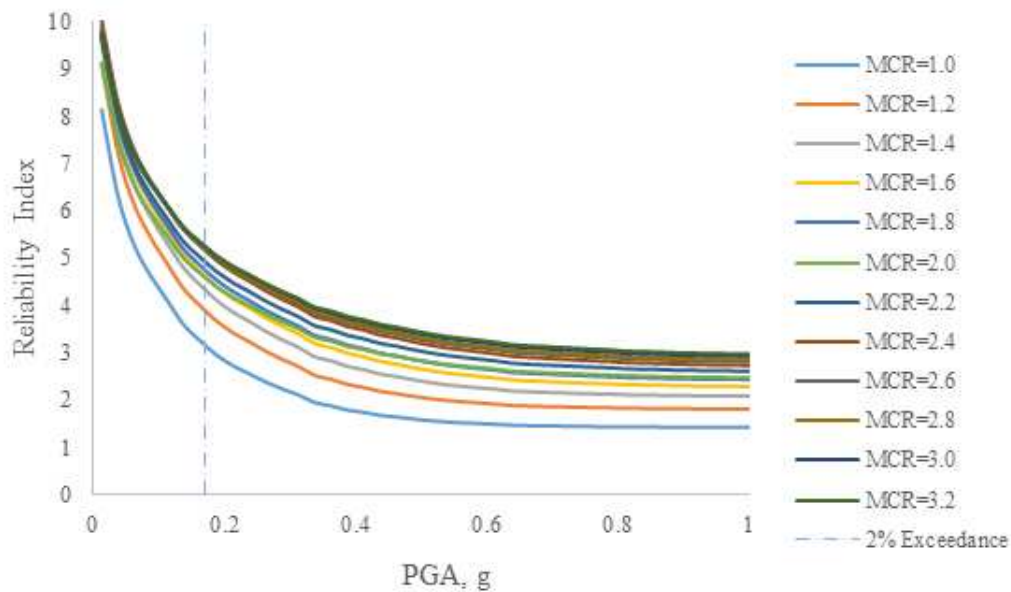


Figure 5.7: Reliability curve of CP for Seismic Zone II

Table 5.4: Target Reliability for IO of various hazard location

| MCR | Target RI for IO | Achieved RI Zone II | Achieved RI Zone III | Achieved RI Zone IV | Achieved RI Zone V |
|-----|------------------|---------------------|----------------------|---------------------|--------------------|
| 1 | 1 | 2.3 | 1.85 | 1.45 | 0.5 |
| 1.2 | 1 | 2.35 | 2 | 1.6 | 0.54 |
| 1.4 | 1 | 2.4 | 2.2 | 1.7 | 0.6 |
| 1.6 | 1 | 2.5 | 2.25 | 1.75 | 0.62 |
| 1.8 | 1 | 2.6 | 2.3 | 1.8 | 0.65 |
| 2 | 1 | 2.65 | 2.35 | 1.85 | 0.7 |
| 2.2 | 1 | 2.7 | 2.4 | 1.92 | 0.73 |
| 2.4 | 1 | 2.75 | 2.45 | 1.96 | 0.77 |
| 2.6 | 1 | 2.85 | 2.48 | 1.98 | 0.8 |
| 2.8 | 1 | 2.95 | 2.54 | 2.02 | 0.86 |
| 3 | 1 | 3.15 | 2.58 | 2.07 | 0.9 |
| 3.2 | 1 | 3.2 | 2.6 | 2.12 | 0.92 |

Table 5.5: Target Reliability for SD of various hazard location

| MCR | Target RI for SD | Achieved RI Zone II | Achieved RI Zone III | Achieved RI Zone IV | Achieved RI Zone V |
|-----|------------------|---------------------|----------------------|---------------------|--------------------|
| 1 | 2 | 3.2 | 2.9 | 1.55 | 0.85 |
| 1.2 | 2 | 3.5 | 3.3 | 1.95 | 1.05 |
| 1.4 | 2 | 3.7 | 3.6 | 2.2 | 1.2 |
| 1.6 | 2 | 3.85 | 3.7 | 2.4 | 1.3 |
| 1.8 | 2 | 3.95 | 3.75 | 2.45 | 1.35 |
| 2 | 2 | 4.1 | 3.84 | 2.5 | 1.4 |
| 2.2 | 2 | 4.15 | 3.9 | 2.65 | 1.52 |
| 2.4 | 2 | 4.2 | 3.96 | 2.8 | 1.65 |
| 2.6 | 2 | 4.25 | 4 | 2.9 | 1.79 |
| 2.8 | 2 | 4.3 | 4.15 | 2.92 | 1.83 |
| 3 | 2 | 4.5 | 4.3 | 2.94 | 1.94 |
| 3.2 | 2 | 4.6 | 4.35 | 2.95 | 2.01 |

Table 5.6: Target Reliability for CP of various hazard location

| MCR | Target RI for CP | Achieved RI Zone II | Achieved RI Zone III | Achieved RI Zone IV | Achieved RI Zone V |
|-----|------------------|---------------------|----------------------|---------------------|--------------------|
| 1 | 3 | 3.1 | 2.85 | 1.85 | 1.5 |
| 1.2 | 3 | 3.9 | 3.5 | 2.45 | 1.9 |
| 1.4 | 3 | 4.4 | 4.1 | 2.9 | 2.3 |
| 1.6 | 3 | 4.5 | 4.2 | 3.15 | 2.45 |
| 1.8 | 3 | 4.65 | 4.35 | 3.2 | 2.55 |
| 2 | 3 | 4.8 | 4.5 | 3.22 | 2.85 |
| 2.2 | 3 | 4.85 | 4.55 | 3.3 | 2.97 |
| 2.4 | 3 | 5 | 4.6 | 3.45 | 3.04 |
| 2.6 | 3 | 5.1 | 4.75 | 3.65 | 3.1 |
| 2.8 | 3 | 5.15 | 4.82 | 3.73 | 3.16 |
| 3 | 3 | 5.2 | 4.85 | 3.85 | 3.2 |
| 3.2 | 3 | 5.2 | 4.9 | 3.9 | 3.25 |

Table 5.7: Suggested MCR for various hazard Location

| Location | MCR | | |
|----------|-----|-----|-----|
| | IO | SD | CP |
| Zone II | 1 | 1 | 1 |
| Zone III | 1 | 1 | 1.2 |
| Zone IV | 1 | 1.4 | 1.6 |
| Zone V | NIL | 3.2 | 2.4 |

5.7 Summary

Fragility analysis show that as the MCR value increases the probability of exceedance decreases proportionately. Reliability index of a building depends on MCR values. As the MCR increases the reliability also increases. In order to obtain as estimate of minimum value of MCR required in a building, the achieved values of reliability is compared with the target values of reliability indices. As the seismic zone increases the MCR value also shall be increased to achieve a target reliability. The minimum values of MCRs required for the four storeyed building to achieve the target reliability at CP level are 1.0, 1.2, 1.6 and 2.4 for seismic zones of II, III, IV and V. The minimum values of MCRs required to achieve the target reliability at SD level are 1.0, 1.0, 1.4 and 3.2 for seismic zones of II, III, IV and V. However, the building is failed to achieve the target reliability for IO level at seismic zone V.

Chapter 6

Conclusions

6.1 Summary and Conclusions

A detailed literature review on the MCR proposed by various international codes and previous literature showed discrepancies in the values of MCR. Hence the objectives of the thesis are identified as to study the behavior of buildings with various values of MCR, to develop a simplified method for the calculation of MCR, to find the reliability of buildings designed for various values of MCR and to propose minimum values of MCR to achieve the target reliabilities. The salient conclusions of the present study is as follows.

- The MCR values is found to have significant effect on the seismic performance of frames. The sequence of formation of plastic hinges is greatly influenced by the MCR values.
- The range of axial force in the typical building frames ranging from four to ten storey are found out. The range of axial force is found to be 0.1 - 0.4 for exterior column and 0.06-0.23 for interior column.
- The values of minimum moment capacity for an existing building is calculated by both methods. The minimum moment carrying capacity can be conservatively determined to be about 0.8 times the moment capacity at zero axial force in a column.
- Fragility analysis show that as the MCR value increases the probability of exceedance decreases proportionately. Reliability index of a building depends on MCR values. As the MCR increases the reliability also increases.

- As the seismic zone increases the MCR value also shall be increased to achieve a target reliability. The minimum values of MCRs required for the four storeyed building to achieve the target reliability at CP level are 1.0, 1.2, 1.6 and 2.4 for seismic zones of II, III, IV and V. The minimum values of MCRs required to achieve the target reliability at SD level are 1.0, 1.0, 1.4 and 3.2 for seismic zones of II, III, IV and V. However, the building is failed to achieve the target reliability for IO level at seismic zone V.

6.2 Future Research Scope

All the research carried out in this research is based on 2D regular framed building, so irregularity in plan as well elevation may consider for future scope. Only one earthquake data has taken for analysis for each building. More earthquake data for individual building also can consider in future. The MCR has taken constant throughout all joints of the floor of the building. But storey wise variation of MCR also can be study.

APPENDIX-A

Table 6.1: Seismic Hazard Zone V

| Zone V | Long (^o N) | Lat. (^o N) | PGA 475 Yr | PGA 2475Yr | PGA 4975Yr | PGA 9975Yr |
|-----------|---------------------------|---------------------------|---------------|---------------|---------------|---------------|
| Bhuj | 70.2 | 24.4 | 0.0789 | 0.149 | 0.1857 | 0.2238 |
| Guwahati | 91.7 | 26.1 | 0.2357 | 0.3795 | 0.4313 | 0.5213 |
| Imphal | 93.8 | 24 | 0.3251 | 0.4869 | 0.5592 | 0.6426 |
| Mandi | 76.9 | 31.7 | 0.1321 | 0.2724 | 0.3533 | 0.451 |
| Srinagar | 74.8 | 34.1 | 0.0888 | 0.1856 | 0.2406 | 0.3066 |
| Tejpur | 92.8 | 26.6 | 0.2528 | 0.3958 | 0.4512 | 0.5467 |
| Darbhanga | 85.9 | 26.1 | 0.0678 | 0.1319 | 0.1637 | 0.2036 |

Table 6.2: Seismic Hazard Zone IV

| Zone V | Long (^o N) | Lat. (^o N) | PGA 475 Yr | PGA 2475Yr | PGA 4975Yr | PGA 9975Yr |
|------------|---------------------------|---------------------------|---------------|---------------|---------------|---------------|
| Amritsar | 74.8 | 31.6 | 0.0307 | 0.0624 | 0.0802 | 0.1019 |
| Chandigarh | 76.8 | 30.7 | 0.1006 | 0.2074 | 0.2659 | 0.3377 |
| Darjeeling | 88.3 | 27.0 | 0.1833 | 0.3598 | 0.4447 | 0.5538 |
| Gangtok | 88.6 | 27.3 | 0.1833 | 0.3461 | 0.4177 | 0.5261 |
| Delhi | 77.2 | 28.6 | 0.0751 | 0.1727 | 0.2183 | 0.2887 |
| Nainital | 79.5 | 29.4 | 0.1847 | 0.3384 | 0.4122 | 0.4997 |
| Roorkee | 77.9 | 29.8 | 0.1009 | 0.2275 | 0.291 | 0.3875 |
| Simla | 77.2 | 31.1 | 0.1288 | 0.2671 | 0.3441 | 0.4251 |

Table 6.3: Seismic Hazard Zone III

| Zone V | Long (^o N) | Lat. (^o N) | PGA 475 Yr | PGA 2475Yr | PGA 4975Yr | PGA 9975Yr |
|-------------|---------------------------|---------------------------|---------------|---------------|---------------|---------------|
| Agra | 78 | 27.2 | 0.0578 | 0.1428 | 0.1863 | 0.2587 |
| Asansol | 86.9 | 23.7 | 0.0691 | 0.1377 | 0.1749 | 0.2168 |
| Bhubaneswar | 85.8 | 20.3 | 0.0252 | 0.0419 | 0.05 | 0.0589 |
| Calicut | 75.8 | 11.2 | 0.0491 | 0.0988 | 0.1307 | 0.1701 |
| Chennai | 80.2 | 13.1 | 0.037 | 0.0631 | 0.0748 | 0.0871 |
| Goa | 74.1 | 15.3 | 0.0351 | 0.0709 | 0.0931 | 0.1213 |
| Mumbai | 72.8 | 19.0 | 0.0654 | 0.1296 | 0.1661 | 0.2102 |
| Nasik | 73.8 | 20.0 | 0.0302 | 0.0571 | 0.074 | 0.0939 |
| Surat | 72.8 | 21.2 | 0.0388 | 0.0813 | 0.106 | 0.1341 |
| Kalapakkam | 80.1 | 12.5 | 0.0495 | 0.0923 | 0.1134 | 0.1357 |
| Kolkata | 88.4 | 22.6 | 0.0957 | 0.2025 | 0.2555 | 0.3289 |

Table 6.4: Seismic Hazard Zone II

| Zone V | Long (^o N) | Lat. (^o N) | PGA 475 Yr | PGA 2475Yr | PGA 4975Yr | PGA 9975Yr |
|---------------|---------------------------|---------------------------|---------------|---------------|---------------|---------------|
| Allahabad | 81.8 | 25.4 | 0.0291 | 0.0693 | 0.0933 | 0.1331 |
| Bangalore | 77.6 | 13.0 | 0.0239 | 0.0383 | 0.045 | 0.052 |
| Bhopal | 77.4 | 23.3 | 0.0283 | 0.0558 | 0.0698 | 0.0879 |
| Hydrabad | 78.5 | 17.4 | 0.0249 | 0.0494 | 0.0634 | 0.079 |
| Jaipur | 75.8 | 26.9 | 0.0695 | 0.1653 | 0.2144 | 0.2935 |
| Mysore | 76.6 | 12.3 | 0.0464 | 0.0776 | 0.0923 | 0.1078 |
| Nagpur | 79 | 21.1 | 0.0387 | 0.0683 | 0.0823 | 0.0973 |
| Tiruchirupali | 78.7 | 10.8 | 0.0334 | 0.0649 | 0.0828 | 0.1033 |
| Raipur | 81.6 | 21.2 | 0.0105 | 0.0162 | 0.0188 | 0.0214 |
| Pondicherry | 79.8 | 11.9 | 0.076 | 0.1522 | 0.1897 | 0.2293 |
| Vishakapatnam | 83.2 | 17.7 | 0.0269 | 0.039 | 0.0448 | 0.051 |

APPENDIX-B

Table 6.5: Column Section Details for Estimating MCR

| MCR | Width | Depth | Reinforcement |
|-----|-------|-------|-----------------|
| 1.0 | 0.278 | 0.278 | 8 NOS 20 ϕ |
| 1.2 | 0.303 | 0.303 | 8 NOS 20 ϕ |
| 1.4 | 0.324 | 0.324 | 8 NOS 20 ϕ |
| 1.6 | 0.345 | 0.345 | 8 NOS 20 ϕ |
| 1.8 | 0.364 | 0.364 | 8 NOS 20 ϕ |
| 2.0 | 0.383 | 0.383 | 8 NOS 20 ϕ |
| 2.2 | 0.400 | 0.400 | 8 NOS 20 ϕ |
| 2.4 | 0.417 | 0.417 | 8 NOS 20 ϕ |
| 2.6 | 0.432 | 0.432 | 8 NOS 20 ϕ |
| 2.8 | 0.444 | 0.444 | 8 NOS 20 ϕ |
| 3.0 | 0.460 | 0.460 | 8 NOS 20 ϕ |
| 3.2 | 0.472 | 0.472 | 8 NOS 20 ϕ |

Table 6.6: Floor Beam Section Details for Estimating MCR

| SL No | Width | Depth | Reinforcement |
|-------|-------|-------|---|
| 1 | 0.250 | 0.350 | 6 NOS 16 ϕ (Top) 4 NOS 16 ϕ (Bottom) |

Table 6.7: Roof Beam Section Details for Estimating MCR

| SL No | Width | Depth | Reinforcement |
|-------|-------|-------|---|
| 1 | 0.250 | 0.350 | 4 NOS 16 ϕ (Top) 3 NOS 16 ϕ (Bottom) |

References

- [1] Paulay T, Park R, and Priestley M J N. Reinforced concrete beam-column joints under seismic actions. *ACI Journal*, pages 585–593, 1978.
- [2] Murthy C V R, Goswami R, Vijayanarayanan A R, and Mehta V V. Some concepts in earthquake behaviour of buildings. http://www.iitk.ac.in/nicee/IITK-GSDMA/EBB_001_30May2013.pdf, 2013.
- [3] IS:13920:2014. Draft code of ductile detailing of reinforced concrete structures subjected to seismic forces- code of practice. *Bureau of Indian Standards, and New Delhi*, 1993.
- [4] Sugano S, Nagashima T, Kimura H, Hara M, Sawamura M, and Yamamoto M. Seismic design and behaviour of a thirty storey reinforced concrete building. *Ninth world conference on earthquake engineering*, vol-v(1), August, and 1988.
- [5] Nakashima M and Sawaizumi S. Column-to-beam strength ratio required for ensuring beam-collapse mechanisms in earthquake responses of steel moment frames. *Proceedings of the 12th World Conference on Earthquake Engineering*, 2000.
- [6] Dooley K L and Bracci J M. Seismic evaluation of column-to-beam strength ratios in reinforced concrete frames. *ACI Structural Journal*, 98(6):843–851, 2001.
- [7] Hibino Y and Ichinose T. Effects of column-to-beam strength ratio on seismic energy distribution in steel frame structures. *Journal of Structural Engineering*, 51B:277–284, 2005.
- [8] Jain S K, Ingle R K, and Mondal G. Proposed codal provisions for design and detailing of beam-column joints in seismic regions. *Indian Concrete Journal*, August 2006.
- [9] George S S and Varghese V. *General Concepts of Capacity Based Design*, volume Volume-1, and Issue-2. July 2012.
- [10] Fox M J, Sullivan T J, and Beyer K. *Capacity Design of Coupled RC Walls*. Taylor & Francis, March 2014.

-
- [11] Aci-318-02. *Building Code Requirements for Structural Concrete (ACI 318M-02) and Commentary (ACI 318RM-02)*, ACI Committee 318, 2002.
- [12] EN 1998-1-3:2003. Design provisions for earthquake resistant structures-part 1: General rules, seismic actions and rules for building. 2003.
- [13] NZS 3101. Concrete structures standard, part 1: The design of concrete structures. *New Zealand Standard*, 1995.
- [14] NZS 3101. Concrete structures standard, part 2: Commentary on the design of concrete structures. *New Zealand Standard*, 1995.
- [15] IS:13920:1993. Ductile detailing of reinforced concrete structures subjected to seismic forces-code of practice. *Bureau of Indian Standards, and New Delhi*, 1993.
- [16] IS:13920:2014 Draft. First revision of is 13920 concrete structures standard, part 2: Commentary on the design of concrete structures. *Bureau of Indian Standards, and New Delhi*, 2014.
- [17] SAP2000. Integrated finite element analysis and design of structures. *CSI, Berkeley California*, v-16.1, 2014.
- [18] Bracci J M., Kunnath S K, and Reinhom A M. Seismic performance and retrofit evaluation of rc structures. *ST Division, and ASCE*, 123(1)(3-10), 1997.
- [19] Tso W K and Moghadam A S. Pushover procedure for seismic of buildings. *Progress in Struct. Eng. and Mater*, 1(3)(337-344), 1998.
- [20] Rahul R, Limin J, and Atila Z. pushover analysis of a 19 story concrete shear wall building. *13th world conference on Earthquake Engineering*, 2004.
- [21] Ho J C M and Kwan A K H. Flexural ductility assessment and concurrent flexural strength and ductility design of reinforced concrete beams. *The 14th World Conference on Earthquake Engineering, Beijing, China*, October 12-17, and 2008.
- [22] Lupoi G. Fragility analysis of the seismic response of freestanding equipment,ph.d thesis. *European School of Advanced studies in Reduction of Seismic Risk-Rose school*, 2005.
- [23] Ellingwood B R. Earthquake risk assessment of building structures. *Reliability Engineering and System Safety*, 74(3)(251-262), 2001.
- [24] Lagaros N D. Probabilistic fragility analysis: A tool for assessing design rules of rc buildings. *Earthquake engineering and engineering vibration*, 7(1)(4556), 2008.

- [25] Celik O C and Ellingwood B R. Seismic fragilities for non-ductile reinforced concrete frames-role of aleatoric and epistemic uncertainties. *Structural Safety*, 32(1)(1-12), 2010.
- [26] Rajeev P and Tesfamariam S. Seismic fragilities for reinforced concrete buildings with consideration of irregularities. *Structural Safety*, 39(1-3), 2012.
- [27] Pragalath H D C. Reliability based seismic design of open ground storey framed buildings. *PhD Thesis, National Institute of Technology Rourkela, India*, 2015.
- [28] FEMA356. Nehr p guidelines for the seismic rehabilitation of buildings. *Federal Emergency Management Agency, Washington DC*, 2000.
- [29] IS:1893. Indian standard criteria for earthquake resistant design of structures, part 1: General provisions and buildings. *Fifth Revision, Bureau of Indian Standards, New Delhi*, 2002.
- [30] SP16. Design aids for reinforced concrete to is: 456-1978. *Bureau of Indian Standards, New Delhi*, 1980.
- [31] Pillai S U and Menon D. Reinforced concrete design-third edition. *McGraw Hill Education India Private Limited*, 2015.
- [32] MATLAB. Matlab - programming software for all kind of problems. <http://www.mathworks.com/>, 2014.
- [33] NDMA. National disaster management authority, government of india. <http://www.ndma.gov.in/en/>, 2015.
- [34] Cornell C A, Jalayer F, Hamburger R O, and Foutch D A. The probabilistic basis for the 2000 sac/fema steel moment frame guidelines. *Journal of Structural Engineering*, 128(4)(526-533), 2002.
- [35] ATC:58. Guidelines for seismic performance assessment of buildings. *Applied Technology Council, Redwood City, CA*, 2012.
- [36] McKay M, Beckman R, and Conover W. A comparison of three methods for selecting values of input variables in the analysis of output from a computer code. *Technometrics*, 21(239245), 1979.
- [37] Opensees. Open system for earthquake engineering simulation, a program for static and dynamic nonlinear analysis of structures. <http://opensees.berkeley.edu/>, 2013.